FINAL TECHNICAL REPORT
September 1, 2006, through August 31, 2007

Project Title: **DEVELOPMENT AND DEMONSTRATION OF ALTERNATE ROOM-AND-PILLAR MINING GEOMETRY IN ILLINOIS – PHASE II**

ICCI Project Number: 06-1/1.1A-3
Principal Investigator: Dr. Y. P. Chugh, Southern Illinois University
Other Investigators: A. Patwardhan, H. Gurley, A. Moharana, J. Pulliam
Project Manager: Dr. Ronald Carty, ICCI

ABSTRACT

The alternate mining geometry concept is a novel method of using unequal pillar sizes with larger pillars in the center and smaller pillars around the edges of a mining section. This allows for more uniform pillar and floor safety factors across the entire width of a mining section while simultaneously achieving a higher extraction ratio. Furthermore, cutting sequence in a panel with alternate geometry can be optimized to realize higher production rate at a lower production cost. In this project, such an 'Alternate Mining Geometry' was demonstrated in a sub-main area of an Illinois mine in cooperation with a coal company. Studies were conducted to: 1) monitor geotechnical and operations performance of a currently practiced regular geometry, 2) develop an 'alternate mining geometry' in cooperation with the mining company, and 3) monitor geotechnical and operational performance of the alternate geometry demonstration area during and after mining. Additional studies were also conducted to investigate possible improvements in productivity achievable from several viable alternate mining geometries.

A 3.2% higher extraction ratio was achieved in the alternate geometry demonstrated. Roof-floor convergence measurements indicated relatively uniform convergence in the alternate geometry area and higher stability around the center of the panel. This was a hypothesized and desired outcome of the study which is beneficial to the overall stability of the panel. The absolute convergence values in the alternate mining geometry were however slightly higher because of higher extraction ratio and weaker floor conditions as determined later from plate load tests. Production simulations indicated that an almost 7% increase in production per unit shift could be achieved in alternate geometry due to the ability to mine single-cut blow-through across smaller outside pillars. A novel approach utilizing dynamic programming techniques was used to generate an optimal cutting sequence which suggested the same, and which corresponded with cut sequences developed by the authors and utilized in production simulations. These cut sequences can be considered to be very close to the true optimal as they were developed with significant efforts and inputs from experienced field personnel and company engineers. Unfortunately during the demonstration the optimal cut sequence to achieve enhanced productivity was not practiced by the mining company. A 50% reduction in out-of-seam dilution from the roof was also documented in the alternate geometry. This is believed to be a result of improved roof stability.

EXECUTIVE SUMMARY

Traditionally, room-and-pillar mining is associated with pillars of uniform size. Though this layout lends itself to simplified mining cut sequences, the extraction ratio is sub-optimal. In such geometry, pillars around the panel center have lower safety factors while pillars around the barrier pillars have higher safety factors. This is because pillar size is based on the highest expected load while pillar loading actually increases from edge pillars (lowest) to central pillars (highest). This leads to a higher risk of roof falls or floor heave in the central entries where the conveyor belt and other critical infrastructure are located.

To overcome the disadvantage of lower extraction ratio and reduced pillar and floor safety factors in the central belt entries, an alternate mining geometry (AMG) concept was developed by the principal investigator (PI). This is a novel concept which utilizes unequal pillar sizes, such that central entries have larger pillars as compared to ones near panel barriers. This allows equalizing pillar safety factors (PSF) and floor safety factors (FSF) across the entire width of a mining section while simultaneously achieving a higher extraction ratio. The term PSF refers to failure of pillar based on coal strength while FSF refers to failure of floor underneath the pillar or foundation failure. Furthermore, cut sequencing in a panel with AMG can be optimized to realize higher production rate at a lower production cost. As a result of improved panel stability, AMG has the potential to reduce ground control costs. Though no accurate economic analyses to assess gains due to better ground control have been conducted yet, it is expected that major economic benefits would accrue due to the lower incidence of roof falls and associated clean-up costs and productivity delays due to falls in belt entries and travel ways.

In this project, SIU researchers, in collaboration with industry professionals developed and demonstrated such an AMG in a sub-mains area of an Illinois mine. The AMG was developed using Finite Element Analysis (FEA) Phase2 software. The AMG demonstration was preceded by installation of convergence and rib stress monitoring stations in a conventional mining geometry (CMG) area. Industrial engineering studies were also conducted to collect data for production simulations. Similar studies were repeated during the AMG demonstration. Following the completion of mining, all the installed convergence and rib stress measurement stations were monitored periodically over 200 days. Visual inspection of the areas was also conducted during measurement visits. An out-of-seam dilution (OSD) measurement program was conducted to quantify the impacts on dilution, if any, due to AMG. The results of these activities are summarized in the following paragraphs.

Development and Demonstration of Alternate Mining Geometry

The CMG at the mine involved 11 pillars on 65-ft centers across the panel width and cross-cuts on 65-ft centers in the direction of advance with 20-ft wide entries and cross-cuts. The AMG utilized three (3) central 65-ft pillars followed by a 60-ft, a 55-ft, and two 50-ft pillars on either side. The FSF and PSF in the CMG were calculated at 1.87 and 4.48 using Vesic-Speck and Holland formulas. The corresponding values obtained

from FEA were 1.6 and 3.2 for FSF and PSF. These numbers are well in excess of the required 1.3 FSF and 1.5 PSF. Hence it is possible to increase extraction ratio without affecting structural stability of the panel or individual pillars within the panel. With the AMG, the FSF and PSF for the smallest 50-ft pillar were calculated as 1.42 and 3.16 using the Vesic-Speck and Holland formulas. The corresponding values of FSF and PSF as obtained from FEA were 1.37 and 2.65. The AMG had relatively uniform PSF values (2.65-3.10) across the panel. The FSFs for the AMG were higher near the center (1.63) than around the edges (1.37) as designed. These values were still higher than required to ensure structural stability of coal pillars. However, it was decided to limit extraction ratio gains to about 3% to achieve operational experience with this AMG before increasing extraction ratio further by lowering safety factors.

The designed CMG and AMG were modeled using the Phase2 FEA software. The safety factors for the CMG indicate that it is over designed around outside entries, but it is also more than adequate around the center of the panel. This would suggest that maintaining the CMG pillar size in the center of the panel while decreasing pillar sizes around the edges should achieve the desired objective of extracting more coal while maintaining ground control stability. This is accomplished in the AMG where the safety factors are higher at the center pillars providing higher stability in the central belt entry and lower but adequate stability around the edges to realize increased extraction.

Geotechnical Monitoring of Conventional and Alternate Mining Geometries

Four (4) rows of convergence stations were established with two (2) in the CMG and two (2) in the AMG 1-2 days after mining each area. These stations were located both in intersections as well as in entries adjacent to pillars of all sizes. There were 14-18 convergence stations per row and each row installed was in the cross-cut behind the last open cross-cut at the time of installation. Monitoring of these stations continued at varying intervals through 200 days after mining. The initial convergence measured 6 days after installation of each row of points in CMG and AMG was 0.0867 of an inch and 0.1356 of an inch. The long-term convergence measurements as measured after 200 days were 0.3467 of an inch and 0.6285 of an inch for CMG and AMG. The coefficient of variation for the 200-day convergence measurements across the panel width for the CMG and AMG was calculated at 45.3% and 36.6%. A lower coefficient of variation across the AMG panel indicates that convergence was more uniform in AMG as compared to CMG. This is expected through design of the AMG pillars where more uniform convergence is targeted to improve roof stability. The long-term and initial convergences in AMG were 80% higher as compared to CMG. The authors believe that the higher convergence observed in AMG was primarily a result of weaker floor conditions. This was later verified through plate loading tests on immediate floor strata both in the CMG and AMG areas.

Rib stress measurement stations were used to monitor incremental stresses in pillar ribs of CMG and AMG. Five (5) rows of rib stress measurement stations (three in CMG and two in AMG) with 4-6 stations per row were installed during mining and were measured periodically. The measured data was utilized to assess incremental vertical and

horizontal stresses in pillar ribs using strain rosette equations. The observations from strain-rosettes did not yield any consistent results for horizontal and shear stress since calculated Poisson's ratio values were typically larger than 0.5, which are physically not possible for a continuum. Authors believe that these results are due to opening up of cracks in coal due to tensile stresses in the lateral direction. However when incremental vertical stress was computed from the strain rosette measurements, both the CMG and AMG showed low and comparable levels of stress.

During a periodic monitoring and measurement visit six (6) months after demonstration, the project staff members observed a small localized area in the AMG section where a moderate amount of rib rash and a very small degree of floor heave had occurred. To scientifically study this problem, plate load tests were conducted in the CMG and AMG demonstration sections. Results of these tests indicated that the floor was significantly weaker on the right side of the AMG section. This result explained the observed localized area of rib stress and minor floor heave. The weak floor was also corroborated by the higher convergence measurements recorded in this area. Hence, the authors concluded that the observed localized areas of high convergence were due to weak floor strata in that area and were not related to AMG.

Productivity and Face Production Cost Impacts of Alternate Mining Geometry

To compare the productivity and related cost benefits resulting from AMG, both CMG and AMG were modeled using the SIU-Suboleski (SSP) Production Model (Chugh et. al. 2005). The CMG model was calibrated with industrial engineering data collected by the project team and the company process improvement team. Since the model production outputs are dependent on the cut sequence utilized, a significant amount of effort was devoted towards developing cut sequences for CMG and AMG that followed the same guiding principles and were unbiased. The developed cut sequences were discussed with mine professionals before they were used in production modeling. The model results clearly indicated that all of the AMGs evaluated outperformed the CMGs in all respects, such as, extraction ratio, productivity and face production cost. The improvements in productivity were projected to be between 5-7% at a corresponding reduction in production cost of 3-4%. The extraction ratio increases were calculated to be 3-5%. The superior productivity and related cost results with the AMG were found to be primarily driven by the ability to mine cross-cuts in the smaller pillars around the edges of the panel with a single-cut (blow-through). In addition to production and cost analysis of the different geometries, delays in each cut in each of the modeled geometries were also compared. Wait times in a mining system can indicate both loss of productive time as well as over-capacity of the system. Frequency distribution plots of the wait times were plotted for different geometries which indicated that the AMG resulted in smaller wait times. Thus the AMG system is a better matched system and results in a lower cost per ton of mined coal.

The actual production numbers during the AMG demonstration were lower than those during CMG but the difference was not statistically significant. The observed lower production was due to the fact that a sub-optimal cut sequence was followed by the

operations staff during the AMG demonstration. Instead of making single-cut blow-through into cross-cuts around the smaller pillars, the cross-cuts were developed by turning cuts from both left and right. This practice is considered worse than the conventional practice of turning and blowing through in two cuts. The reasons for selecting this clearly inferior cut sequence during mining are not known.

Optimized Cut Sequencing

A dynamic programming algorithm was used to solve the problem of scheduling optimized cut sequences. Factors considered in the selection of successive optimum cuts were bolting, ventilation and cable handling. Weights for these factors were assigned based on field experience. The model successfully generated optimum cut sequences that matched the refined cut sequences which were manually developed after several trials and with inputs from experienced field personnel and engineering staff. This model is being improved by enhancing the scientific basis for determining the factor values.

Out-of-Seam Dilution Impacts of Alternate Mining Geometry

To determine the impact of AMG on OSD, a roof and floor dilution measurement program was conducted approximately seven (7) months after demonstration. Due to the hypothesized superior stability of AMG, it was thought that lower OSD may be associated with this geometry. Measurements were conducted across four (4) cross-cuts both in the CMG and AMG areas. Mining height measurements were taken in the entries and cross cuts and the roof, floor and seam measurements were taken on the four faces of all the pillars. The resultant data indicated an almost identical average seam height measurement in both geometries. The average measured floor thickness was also very similar in both CMG and AMG. It was found that there was almost a 2-inch or 50% reduction in the mined roof thickness in the AMG. The mined roof thickness values were found to be different at a statistical significance level greater than 99.9%. Correspondingly, the total mined height was also lower for the AMG. Overall, the results indicated that there was less OSD in AMG. This could be attributed to the overall improved ground stability in the AMG. Benefits arising from lower roof dilution would include lower equipment maintenance, lower production cost, increased preparation plant recovery and efficiency and better product quality.

Summary Outcome of the Project

The field demonstration of AMG concept has indicated that significantly increased production (5-7%) per unit shift, associated with decreased production cost is possible while simultaneously enhancing panel ground stability in similar ground conditions. The project team has advanced the state-of-the-art in analyzing both production and ground stability aspects of AMG. The AMG concepts have been field demonstrated at two mines in Illinois, with long-term geotechnical monitoring. The authors suggest that the coal industry implement these concepts in their mine settings to reduce production cost and improve ground control. The AMG concepts can be further enhanced as experience is gained with more frequent use of AMG.

OBJECTIVES

The goal of this project was to develop and demonstrate an AMG for a sub-main development at a mine in Southern Illinois. The objectives of this demonstration were to achieve:

1. Higher extraction ratio with the AMG.
2. Higher PSF and FSF around the center of the sub-main section that will enhance ground stability of belt and power entries.
3. Higher overall long-term stability of the sub-main area that will preserve the integrity of primary airways.
4. Smaller sub-main foot print area allowing more reserves for panel mining.
5. Higher production and productivity potential through cut sequence optimization.

INTRODUCTION AND BACKGROUND

Traditionally, room-and-pillar mining is associated with pillars of uniform size in both development entries and in panels (Figure 1). Though this layout lends to simplified mining cut sequences, the extraction ratio in the mined-out areas is sub-optimal. In a CMG setting, stresses on pillars are highest around the center and lowest around the edges, thus putting belts and other infrastructure at risk. Safety factors for roof and pillar failures based on coal and floor strengths vary across and along a panel for a given mining geometry. Designs for Illinois coal mines require minimum PSF and FSF to be 1.5 and 1.3, respectively.

To overcome the disadvantage of lower extraction ratio and reduced safety factors around the central belt entries, AMG concepts were proposed to the mining industry. AMGs (Figure 2) have unequal pillar sizes, such that central entries have larger pillars as compared to those adjacent to the barrier pillars. Some AMGs may include a large pillar near the panel edge so that the load on smaller edge pillars can be transferred to the larger pillar. Additional advantages of this system include: (1) increased stability of the entire mining development, (2) higher extraction ratio, (3) increased production per unit shift through mining some cross-cuts with a single-cut (blow-through) and optimization of cutting sequence, and (4) reduced roof fall risk in the central belt entries. Selection of AMGs is based on an optimization procedure that utilizes computed values of loading and strength of pillars spatially in a mining layout, and the load transfer from mined-out areas to unmined areas. Modeled safety factors for CMG and AMGs at a previous demonstration mine in Illinois are shown in Figures 3(a) and 3(b). It is apparent that moving from edge pillars to the center, safety factors decrease for the CMG while they increase for the AMG. Greater safety factors mean that vertical displacement is minimized resulting in less spalling and roof control problems. This is particularly beneficial in the belt entry around the panel center as it reduces the risk of roof falls.

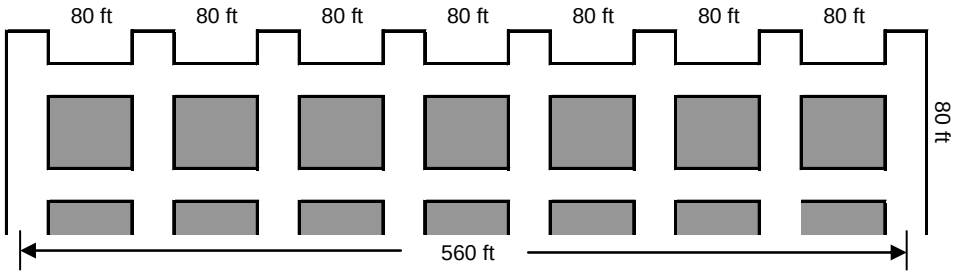

Figure 1. Traditional room-and-pillar mining geometry from a previous demonstration (Chugh et. al., 2004b).

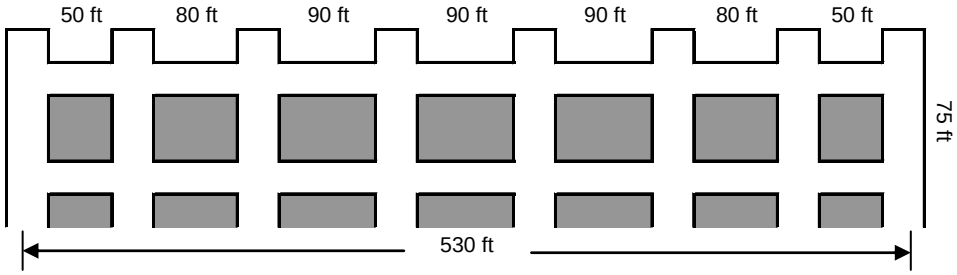

Figure 2. Alternate room-and-pillar mining geometry from a previous demonstration (Chugh et. al., 2004b).

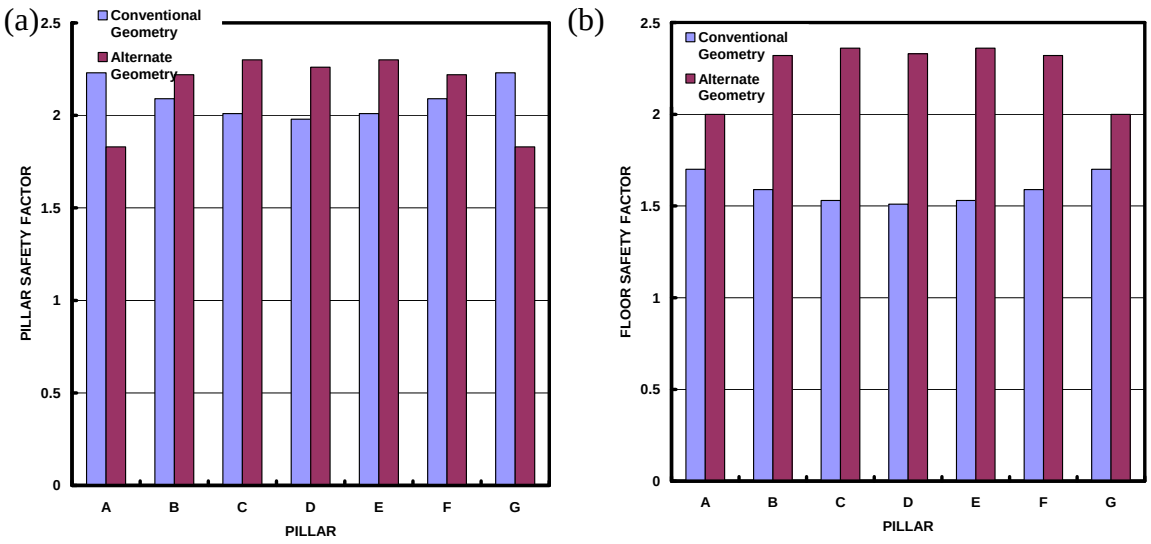

Figure 3. Comparison of (a) PSF and (b) FSF for CMG and AMG (Chugh et. al., 2004b).

Economic Benefits of Alternate Geometry

In addition to delivering a higher extraction ratio, the AMG has the potential for higher production per unit shift and lower ground control costs. Though no accurate economic

analyses to assess gains due to better ground control have been conducted yet, it is expected that major economic benefits would accrue due to the lower incidence of roof falls and associated clean-up costs and fewer production delays due to falls in belt entries and travel ways. It is expected that economic benefits of AMG will result from the following:

1. Increased extraction ratio - Extraction ratios in typical mains and sub-mains mined in Illinois vary from 46-48%. Use of AMG designs can help mines to increase their extraction ratios by about 3%. Cost advantages accrue because of higher returns on the same feet of development advance. Also, the production cost of the incremental coal is expected to be low.
2. Decreased footprint of main and sub-main entries - Smaller edge pillars will narrow the total width of main or sub-main sections. Not only will this increase the overall safety factor of the section but it also implies that a smaller portion of the coal reserve is committed to developing mains and sub-mains. This frees up coal reserves for panel mining where extraction ratios are higher and production costs are lower.
3. Improved production per unit shift through cut sequence optimization - Smaller edge pillars could potentially change the number of two-cut blow-through cross-cuts into cross-cuts mined in a single-cut while simultaneously decreasing haul distances due to decreased footprint.
4. Reduced convergence in central mining entries - Reduced convergence reduces the risk of roof falls. Of particular importance may be the reduction in the frequency of roof falls around the central belt entry, where roof falls can completely shut down production.
5. Reduced rib-spalling - Higher PSF and FSF values around central entries should lead to reduced rib spalling. This effectively increases the usable portion of the entry width and reduces time and cost associated with cleaning up the sloughed material.
6. Increased stability of long-term mine development - AMG is expected to provide higher long-term stability which should be beneficial for mains and sub-mains which must stand for longer periods of time.

EXPERIMENTAL PROCEDURES

This project was proposed to collect baseline performance data on CMG with uniform size pillars currently used in a sub-main and compare it to an AMG with non-uniform size pillars. The associated geologic, geotechnical, and mine environment data in both geometries were also collected and compared. Three major experimental and modeling procedures were used: 1) Establishing convergence stations, 2) Establishing rib stress measurement stations, and 3) FEA modeling of CMG and AMG.

Convergence Stations

Convergence stations monitor movement between roof and floor. A schematic diagram of a convergence station used in this study is given in Figure 4. For installation of these stations, a plumb bob was hung from a roof bolt to accurately mark a point vertically

below it. A hole 1.5 feet deep was drilled into the floor using a Schroeder drill (Figure 5). A convergence pin (1-foot long and 5/8-inch diameter) with polished head was then grouted into the hole in the floor using resin glue. A plastic spacer was inserted over the bolt and the spacer was filled with a sponge-type filling material. The spacer was then covered with a metal ring with a string attached to it. This allowed quick access to the bolt during convergence monitoring.

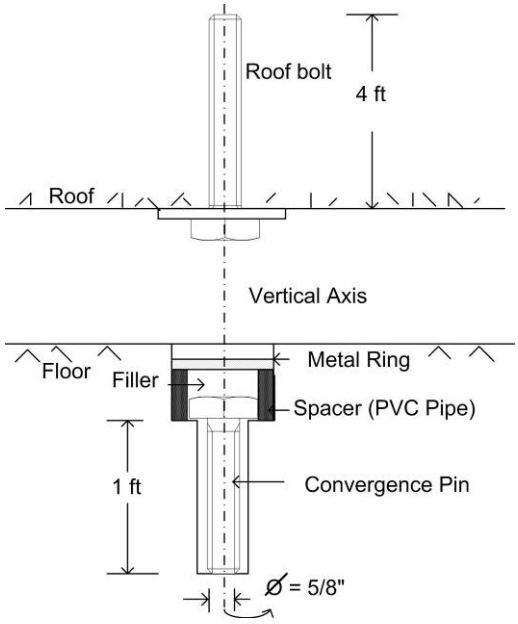

Figure 4. Schematic diagram of a convergence station.

Four (4) rows of such convergence stations were established with two (2) in the CMG and two (2) in the AMG. These stations were located both in intersections as well as in entries adjacent to pillars of all sizes. There were 14-18 convergence stations per row and each row installed was in the cross-cut behind the last open cross-cut at the time of mining and was installed within 1-2 days after mining.

Convergence readings were taken at suitable intervals using an Invar Tube extensometer (Soil Test Inc.). The extensometer consisted of two concentric tubes, one fixed and the other movable. The displacement of the movable tube could be read on a dial gage (0 +/- 0.001 of an inch) to determine total linear distance between the roof and the floor pins below it. Comparison with previous readings was used to determine convergence/divergence values at each point over the time interval.

Rib Stress Measurement Stations

Rib stress measurement stations were used to monitor incremental stresses in pillar ribs of the CMG and AMG. To establish a rib stress measurement station (Figure 6), three holes were drilled as a rectangular rosette and bolts were grouted into each hole. Bolts were 2 feet in length and 5/8-inch in diameter. These bolts were polished at the top and the sides to reduce measurement errors. Five (5) rows of rib stress measurement stations (three in CMG and two in AMG) with 4-6 stations per row were installed. Each row was

installed in the pillars just out bye of the last open cross-cut at the time of mining and within 1-2 days after mining. Horizontal, vertical and diagonal measurements were taken at suitable intervals using a 36-inch long vernier caliper (0 +/- 0.001 of an inch). These data were utilized to assess incremental vertical and horizontal stresses in pillar ribs using strain rosette equations (Goodman, 1980).

Figure 5. Installing convergence points by drilling into the floor using a Schroeder drill.

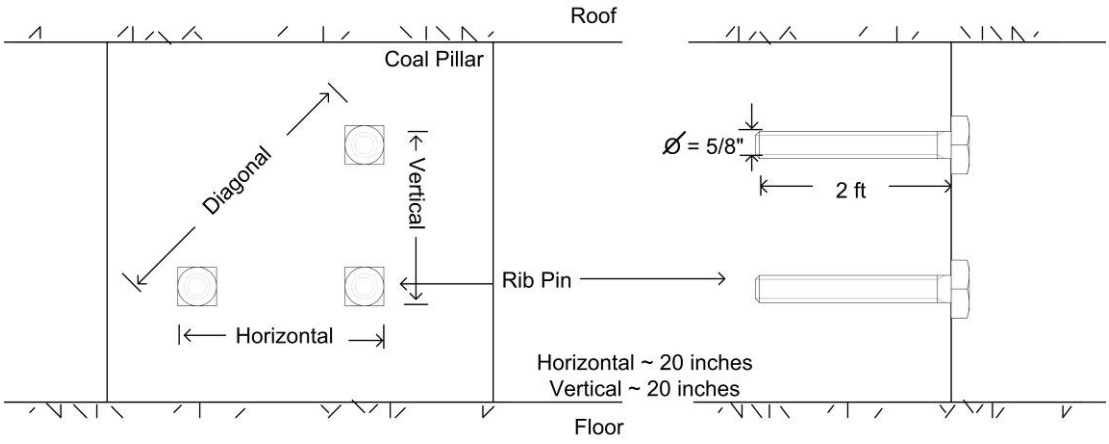

Figure 6. Schematic diagram of a rib-stress measurement strain-rosette station.

Finite Element Analysis (FEA)

Two dimensional models were created using Phase2 (RockScience Inc.) FEA software to model CMG and AMG. Half barrier pillar width of 50 feet was assumed on both sides of the panel. CMG and AMG sections were modeled based on the lithology of boreholes closest to the CMG and AMG demonstration areas. Table 1 gives the lithology of the borehole closest to the area with CMG while Table 2 gives the lithology of the borehole

closest to the AMG. Table 3 gives values of geotechnical parameters for different strata used in FEA models. The models were analyzed with both vertical and horizontal applied stresses. Vertical stress of 325 psi was applied about 80 feet above the coal seam on the model and was simulated as uniform loading on the model. This was calculated as the equivalent vertical stress for two-dimensional modeling. Horizontal stress of 1,000 psi was assumed. This was simulated by setting a displacement in the negative direction due to applied 1,000 psi horizontal stress. This allowed different lithologies to assume different horizontal stresses based on their stiffness. The bottom portion of the model was restrained in the vertical direction, but was allowed to move horizontally. The model was developed with 15,000 uniform three-node triangular elements. The failure analysis was run using linear Mohr-Coulomb failure criterion. Figure 7 shows a screenshot for the ground control model for an AMG design.

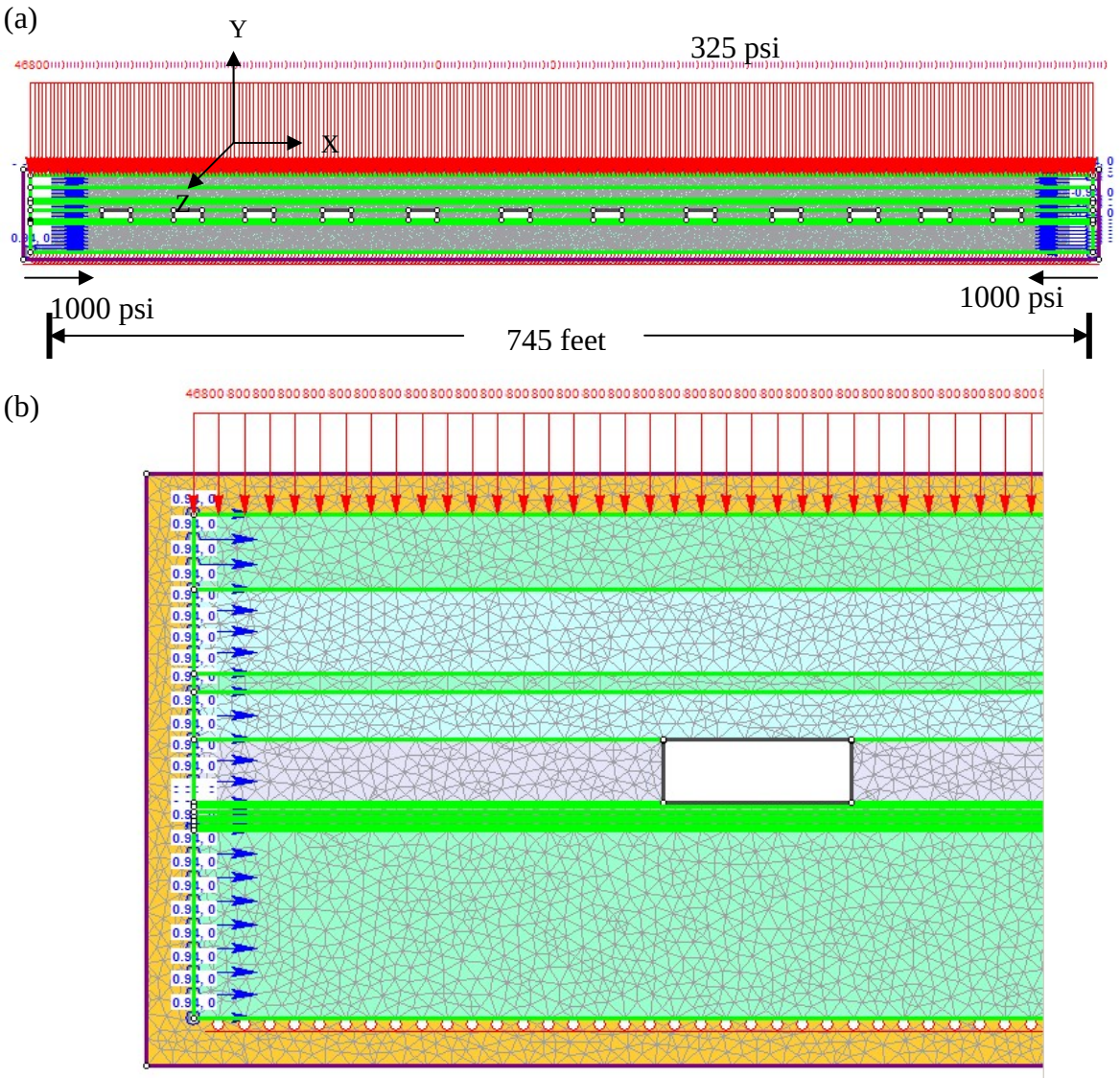

Figure 7. Screenshot of FEA model of AMG using Phase2 FEA software; (a) whole model, and, (b) zoomed view of the edge showing boundary conditions.

Displacement is shown in feet and the loading in psf.

Table 1. Borehole lithology around the CMG area.

Gray Green Silty Shale	6.6 ft	Roof
Limey Shale	8.5 ft	
Gray Limestone	3 ft	
Black Shale	3.2 ft	
Dark Fossil Shale	1.1 ft	
Black Limey Shale	3.8 ft	
Dark Fossil Limestone	2.8 ft	
Black Shale	2.1 ft	
Black Shale w/Sulfur	1.1 ft	
Coal	6.9 ft	Coal
Claystone	0.6 ft	Floor
Shale w/ Limestone Nodules	0.5 ft	
Gray Limestone	2 ft	

Table 2. Borehole lithology around the AMG area.

Limestone	4.1 ft	Roof
Green Gray Striped Shale	3.8 ft	
Limestone	3.9 ft	
Black Shale	2.6 ft	
Core Loss	0.9 ft	
Dark Fossil Shale	1.9 ft	
Dark Fossil Limestone	1.3 ft	
Dark Fossil Shale	3 ft	
Dark Fossil Limestone	2 ft	
Black Shale w/ Sulfur nodules	1.8 ft	
Black Fossil Shale	0.4 ft	
Black Shale	2.7 ft	
Coal	6.7 ft	Coal
Claystone	1 ft	Floor

Table 3. Geotechnical material properties used in FEA models.

Material	Unit Weight (pcf)	E (kpsi)	μ	Tensile Strength (psi)	Friction Angle (deg)	Cohesion (psi)
Coal	80	150	0.28	100	1	450
Claystone	130	30	0.35	30	1	175
Shale	140	300	0.25	200	25	700
Sandstone	155	900	0.18	400	20	2,000
Limestone	165	700	0.20	400	20	2,000
Competent Clay	140	75	0.30	50	1	250

Mohr-Coulomb Failure Criterion

Mohr-Coulomb criterion is a common failure criterion used to calculate rock (brittle) failure or yielding. It describes the limiting relationship between normal and shear stresses on a plane at failure. This criterion suggests that chances of failure are high when the stress at a point is close to the Mohr's circle envelope. (RocScience, 2006).

The direct shear formulation of the criterion (denoted by the strength envelope in Figure 8) is given by the following equation:

$\tau = c + \sigma_n \tan \phi$

where, c is the cohesive strength of rock,
ϕ is the angle of internal friction for rock,
σ_n is the normal stress on the failure plane, and,
τ is the shear strength of the failure plane

The Phase2 FEA program can also calculate equivalent Mohr-Coulomb parameters for non-linear failure envelopes over a specified stress range. However, linear failure criterion was assumed for all analyses performed here.

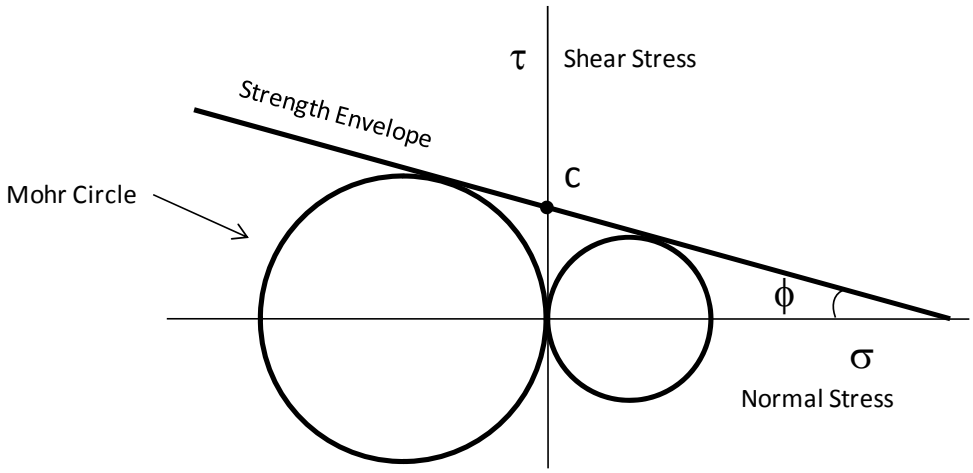

Figure 8. Mohr-Coulomb failure envelope in graphical form. Compression is negative.

Modeling a 3D Mining Geometry using a FEA 2D Model

The 2-D plane strain analysis model geometry extends infinitely in both positive and negative 'z' directions. Such modeling of the CMG and AMG with the overburden vertical stress (σ_v) will assume no cross-cuts in the panel. Therefore, the concept of "equivalent vertical stress" on the panel was used to model the effect of cross-cuts in the mining geometry.

Figure 9 shows the cross-section around a pillar that was modeled in Phase2. The FEA model geometry (Figure 7) was derived from the 3-D geometry of a panel by analyzing the panel across a vertical plane (AA'). Thus, to model the effect of additional extraction in the cross-cuts, the vertical stress on the model was increased by the ratio of the area carrying the load prior to mining to the area of the pillar after mining. In the z-direction, the load was carried by the area EFGH prior to mining and by the area ABCD after mining.

Thus, effective stress on the pillar = $\sigma_v \times \dfrac{\text{area(EFGH)}}{\text{area(ABCD)}}$

$$= \sigma_v \, X \, \frac{(D + E) \, X \, W}{D \, X \, W}$$

where, D = length of the pillar,
W = width of the pillar, and
E = entry width

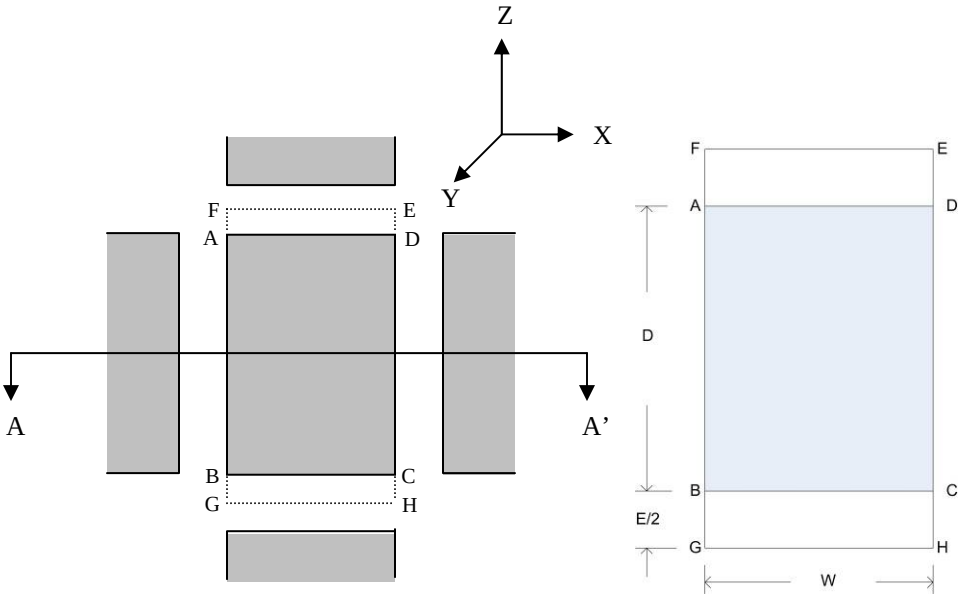

Figure 9. Calculation of equivalent vertical stress.

RESULTS AND DISCUSSION

Task 1: Development of Alternate Geometry for Sub-Main Demonstration at an Illinois Mine

The design of the different AMGs evaluated was based on an optimization procedure that utilized FEA computed values of loading and strength of different sized pillars in a mining layout, and load transfer across pillars and to unmined areas. The analyses also included production modeling, including delays and cost analysis of the proposed mining system. Out of many geometries modeled, two AMG options were considered in depth for this site and are shown in Figures 10 (b) and 10 (c), along with the CMG in Figure 10 (a). Both AMGs achieved the desired benefits of greater extraction ratio, increased ground stability, improved productivity and reduced production cost. The first option (Figure 10 (b)) followed the pattern established in the previous demonstration at another mine in Illinois. It utilized the largest pillars around the panel center with pillar sizes continuously decreasing towards the panel edges. The other option (Figure 10 (c)) utilized the largest pillars around the panel center but also included a slightly larger pillar near each edge of the panel with smaller pillars on either side. These larger pillars were positioned such that the load from the smaller pillars could be effectively arched onto larger pillars and barrier pillars. However, the project team and mine management decided to demonstrate AMG #1 (Figure 10 (b)) at the mine since the previous

demonstration had successfully demonstrated this configuration. This geometry increased the extraction ratio of the panel from 53.3% to 56.5% while reducing the panel footprint from 715 feet to 625 feet. After finalizing the mining geometry to be demonstrated, PSF and FSF values were also calculated using tributary area theory to help mine management in obtaining an experimental permit for field demonstration. Details of the FEA modeling and safety factor calculations for permitting purposes are presented below. A distinct section on productivity comparisons between the two geometries is included after the AMG demonstration section in this report.

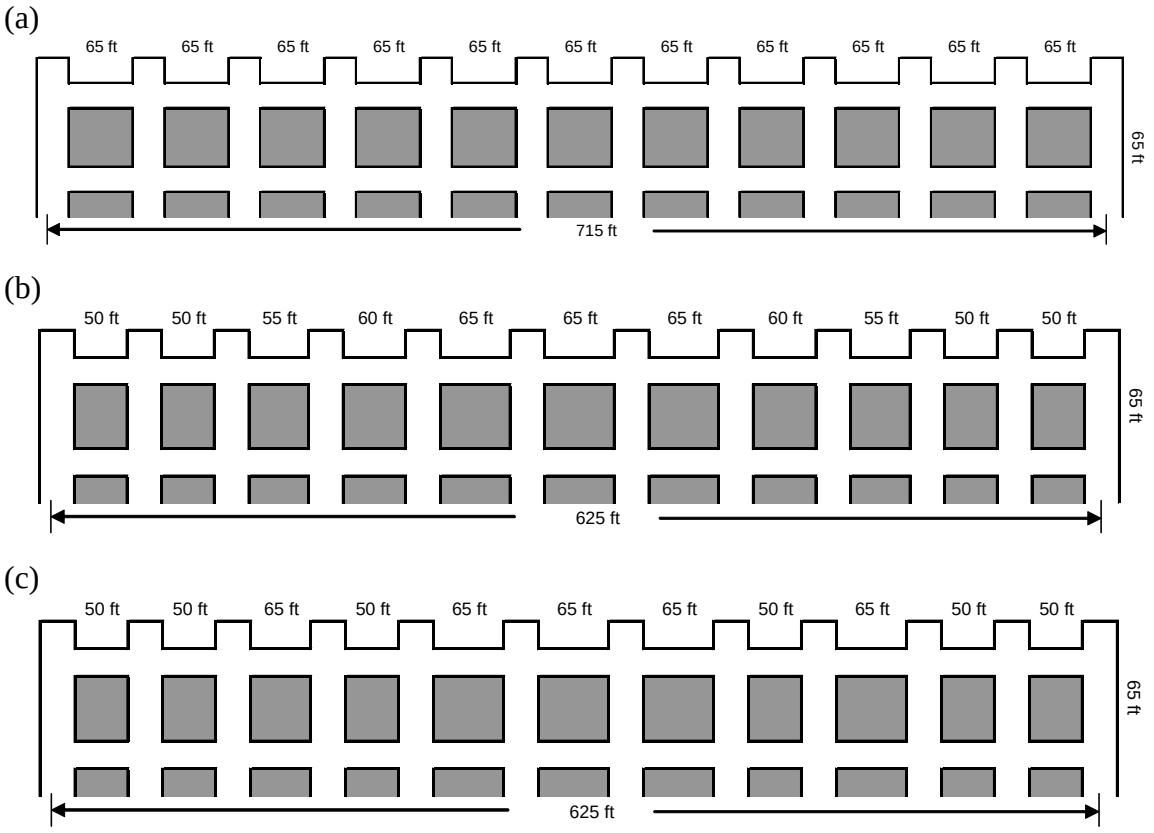

Figure 10. (a) CMG, and, AMG options (b) #1 and (c) #2.

Calculation of Pillar and Floor Safety Factor using Tributary Area Theory (Task 1.1)

To assist the mine management in obtaining an experimental permit for field demonstration, PSF and FSF were calculated using the Vesic-Speck and tributary area approaches (Chugh and Hao, 1992). Vesic-Speck FSF value is a conservative estimate since the angle of internal friction (ϕ) is assumed to be zero, while the value of ϕ typically varies between 15-18 degrees for claystone below the coal seam in Illinois mines. Furthermore, tributary area loading represents maximum loading on pillars. The PSF and FSF were also calculated for each of the various pillar sizes in the AMG shown in Figure 11. For instance, pillar type I is 50-feet x 65-feet (c-c) and calculation of PSF and FSF for it is shown below.

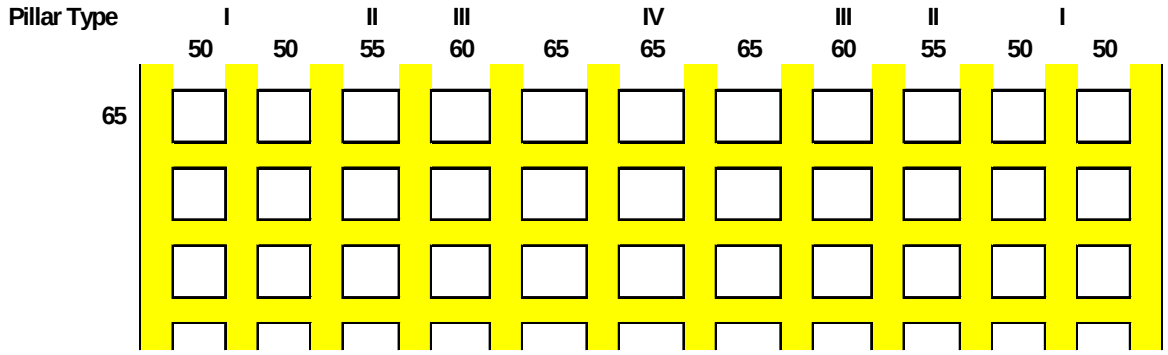

Figure 11. Pillar types of the demonstrated AMG.

Calculation of PSF (Pillar Type I)

Using the Holland formula (Holland, 1964; Holland, 1973), in-situ pillar strength is given by:

In-situ pillar strength (σ_p) = (σ_{cc}) X $\sqrt{\frac{Wp}{h}}$

where Wp = pillar width = 30 feet
h = seam height = 6.5 feet
and σ_{cc} = critical size or in-situ coal strength = 900 psi

Thus, In-situ pillar strength (σ_p) = 900 X $\sqrt{\frac{30}{6.5}}$ = 1,933 psi.

$$PSF = \frac{\sigma_p}{1.1x\frac{D}{1-e}}$$

where D = depth of overburden = 230 feet
e = extraction ratio = 58.5 % (for Type I pillar)

$$\text{Thus, } PSF = \frac{1933}{1.1x\frac{230}{1-0.585}} = 3.16$$

Calculation of FSF (Pillar Type I)

The authors used results of plate loading tests conducted by mine personnel.

Average bearing capacity (based on 9-inch x 9-inch plate loading tests) = 725 psi

Cohesion (S_1) = $\frac{\text{Bearing Capacity}}{N_c^*}$ (Chugh and Hao, 1992)

= 725 / 6.17 = 117 psi,

where, Nc^* = 6.17 (assuming $\phi = 0$)

Ultimate Bearing Capacity (UBC) of Pillar is given by:

$$q_O = S_1 N_m \ ,$$

where, N_m = modified bearing capacity factor

Vesic (1970) proposed the following equation for the determination of N_m:

$$N_m = \frac{KN_C^*(N_C^* + \beta - 1)[(K+1)N_C^{*2} + (1+K\beta)N_C^* + \beta - 1]}{[K(K+1)N_C^* + K + \beta - 1][(N_C^* + \beta)N_C^* + \beta - 1] - (KN_C^* + \beta - 1)(N_C^* + 1)}$$

where, K= ratio of unconfined shear strength of lower hard layer (S_2) to the upper weak layer (S_1)

and, $\beta = \frac{BL}{[2(B+L)H]}$ can be found from the width (B), length (L) and thickness (H) of

the foundation (weak floor). B and L correspond to pillar width (W_p) and pillar length (W_l), respectively.

Thus, UBC = 865 psi

σ_p = 1.1 X D / (1-e) = 610 psi (for Type I pillars)

FSF = 865/ σ_p = 865/610 = 1.42

Table 4 lists calculated FSF and PSF values for different pillars in the AMG. The PSF values are greater than the required 1.5 and FSF values are greater than the required 1.3. Thus, the extraction ratio could be further increased in the AMG. Since limited geologic data was available for the area, it was decided to limit the initial demonstration to a 3% increase in extraction ratio.

FEA Modeling of CMG and AMG (Tasks 1.1 and 1.2)

The CMG and selected AMG were also modeled with Phase2 FEA software using the methodology described previously. Data provided by the company in Table 5 along with the lithology and material properties data summarized in Tables 1-3 were used in modeling and calculations. Safety factors and expected convergence in the entries were analyzed from the model.

Table 4. Safety factors for different pillars in the panel calculated (3-feet weak floor based on lithology data indicating 1-foot of immediate weak floor and 2-feet of weak gray limestone material, 230-feet depth).

Pillar Type	Pillar Width (solid) feet	Pillar Length (solid) feet	Extraction Ratio (%)	Pillar Floor Bearing capacity (psi)	Vesic-Speck Floor Safety Factor	Pillar Safety Factor (Holland)
I	30	45	58.5	865	1.42	3.16
II	35	45	55.9	911	1.59	3.64
III	40	45	53.8	950	1.73	4.07
IV	45	45	52.1	985	1.87	4.48

Table 5. Mining parameter values obtained from company tests and data.

	Parameter	**Value**
1.	Average bearing capacity (based on 9-in. X 9-in. plate loading tests) of immediate floor strata	725 psi
2.	Immediate floor thickness (maximum)	2.33 feet
3.	Moisture content of floor strata	8.0 %
4.	Seam height	6.5 feet
5.	Overburden depth (maximum)	231 feet
6.	Entry width	20 feet
7.	Critical size coal strength (σ_{cc})	900 psi

As shown in Figure 12, the pillar safety factor was calculated by averaging point values along the mid-plane of the pillar. Similarly, the floor safety factor was calculated by averaging point values at a plane 0.5-foot below the pillar.

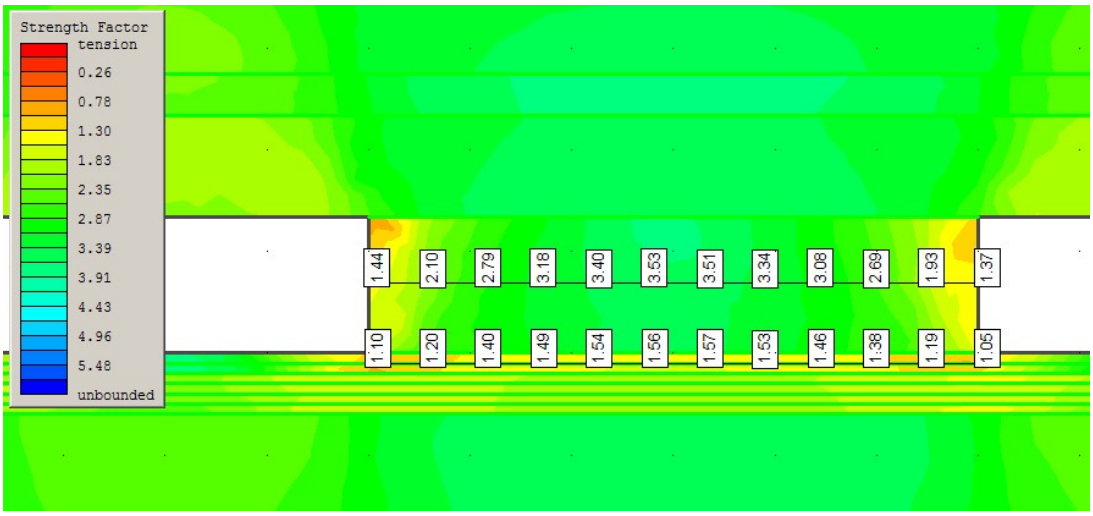

Figure 12. Point values of pillar (mid-plane) and floor (on a plane 0.5-foot below the pillar) safety factors as obtained from the FEA modeling of AMG at the left outside pillar.

Figure 13 shows the averaged FSFs and PSFs across the AMG and CMG panels as obtained from FEA modeling. The safety factors for the CMG indicate that it is over designed around outside entries, but it is also more than adequate around the center of the panel. This would suggest that maintaining the CMG pillar size in the center of the panel while decreasing pillar sizes around the edges should achieve the desired objective of extracting more coal while maintaining ground control stability. This is accomplished in the AMG where the safety factors are higher at the center pillars providing higher stability in the central belt entry and lower but adequate stability around the edges to realize increased extraction. The PSF and FSF values from modeling are also comparable to those obtained using the tributary area approach (Table 6) based upon which the experimental permit was obtained.

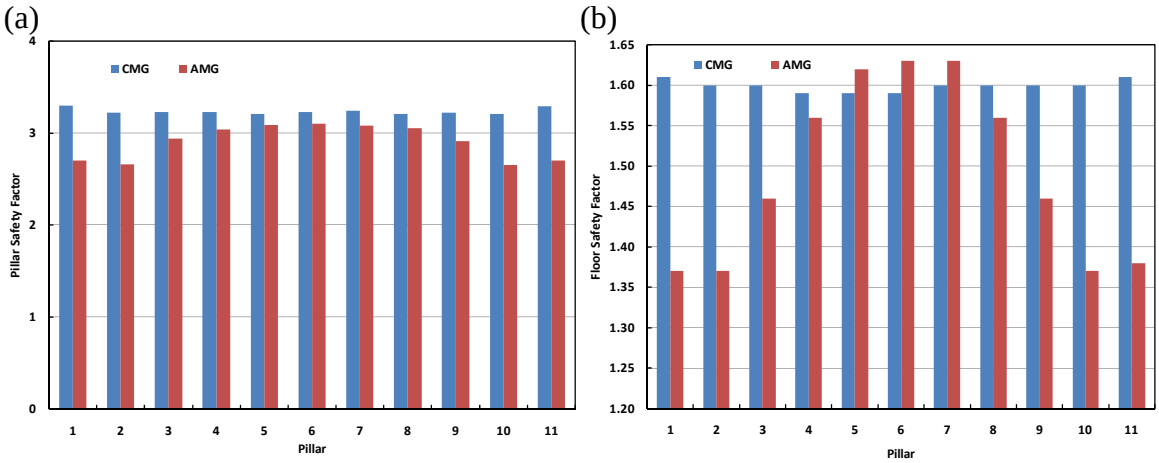

Figure 13. Comparison of safety factors of (a) pillar and (b) floor across a panel for CMG and AMG.

Table 6. Comparison between floor and pillar safety factors in CMG and AMG as obtained from FEA and the tributary area approach.

Pillar	Floor Safety Factor			Pillar Safety Factor		
	CMG-FEA	AMG-FEA	AMG-Vesic-Speck	CMG-FEA	AMG-FEA	AMG-Holland
1	1.61	1.37	1.42	3.30	2.7	3.16
2	1.6	1.37	1.42	3.22	2.66	3.16
3	1.6	1.46	1.59	3.23	2.94	3.64
4	1.59	1.56	1.73	3.23	3.04	4.07
5	1.59	1.62	1.87	3.21	3.09	4.48
6	1.59	1.63	1.87	3.23	3.1	4.48
7	1.6	1.63	1.87	3.24	3.08	4.48
8	1.6	1.56	1.73	3.21	3.05	4.07
9	1.6	1.46	1.59	3.22	2.91	3.64
10	1.6	1.37	1.42	3.21	2.65	3.16
11	1.61	1.38	1.42	3.29	2.7	3.16

Alternate Mining Geometry Demonstration (Task 1.3)

The AMG demonstration area in the sub-mains of an Illinois mine along with the comparative CMG area is shown in Figure 14. Two rows of convergence monitoring stations and three rows of rib rosettes were installed in the CMG area prior to the transition into AMG. Particular locations of these installations are also shown in Figure 14. Similar convergence and rib points were installed in two rows in the AMG demonstration area. The convergence and rib points were installed one cross-cut behind the last open cross-cut from the face and 1-2 days after mining in all instances. This was done to maintain a consistency in the timing of installation so that the time elapsed since mining that particular point to the installation of the points would be consistent. The convergence and rib points were monitored periodically after approximately 1, 2, 4, 6, 8, 10, 15, 35, 90, 120 and 200 days from installation.

(a)

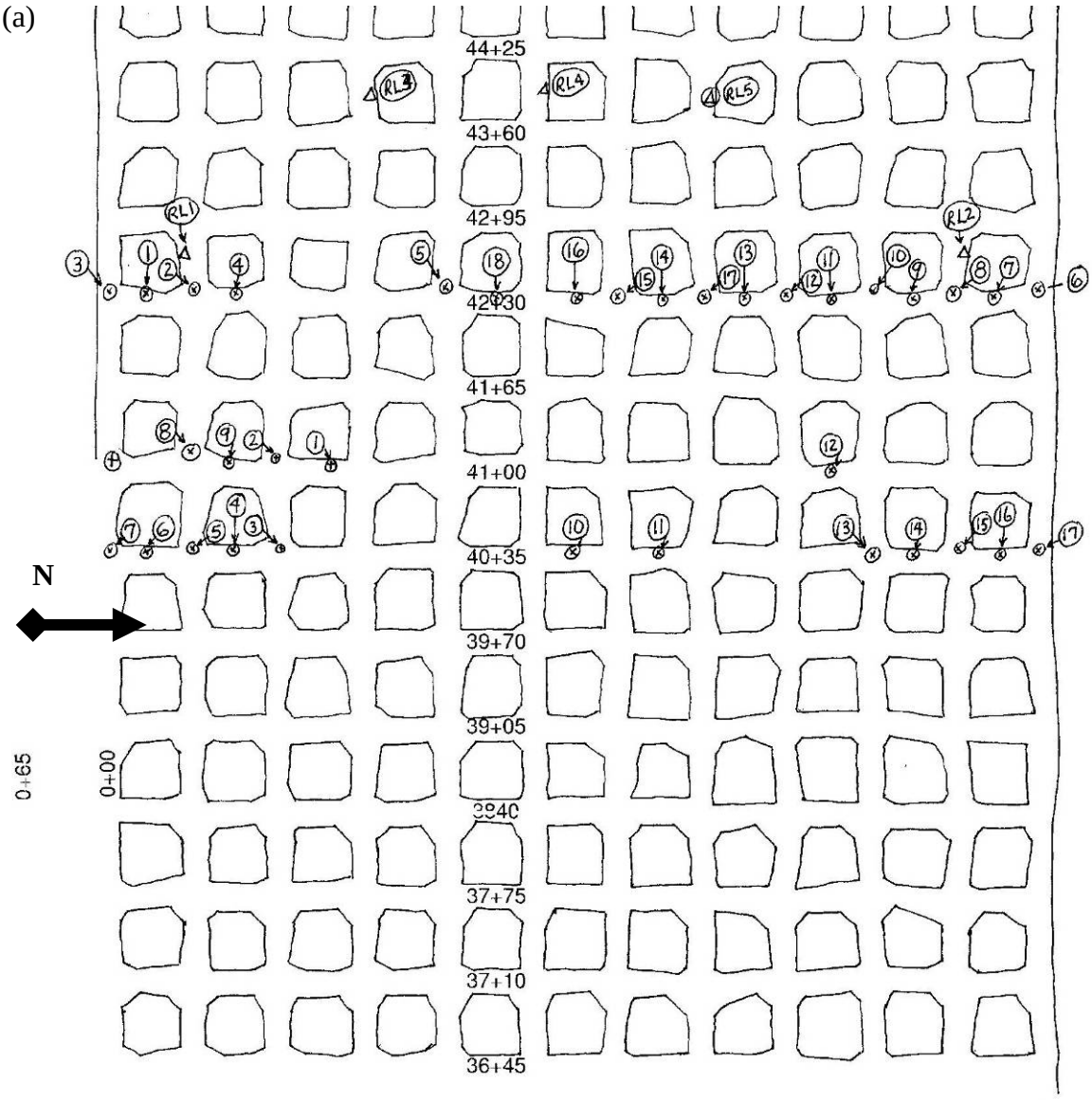

(b)

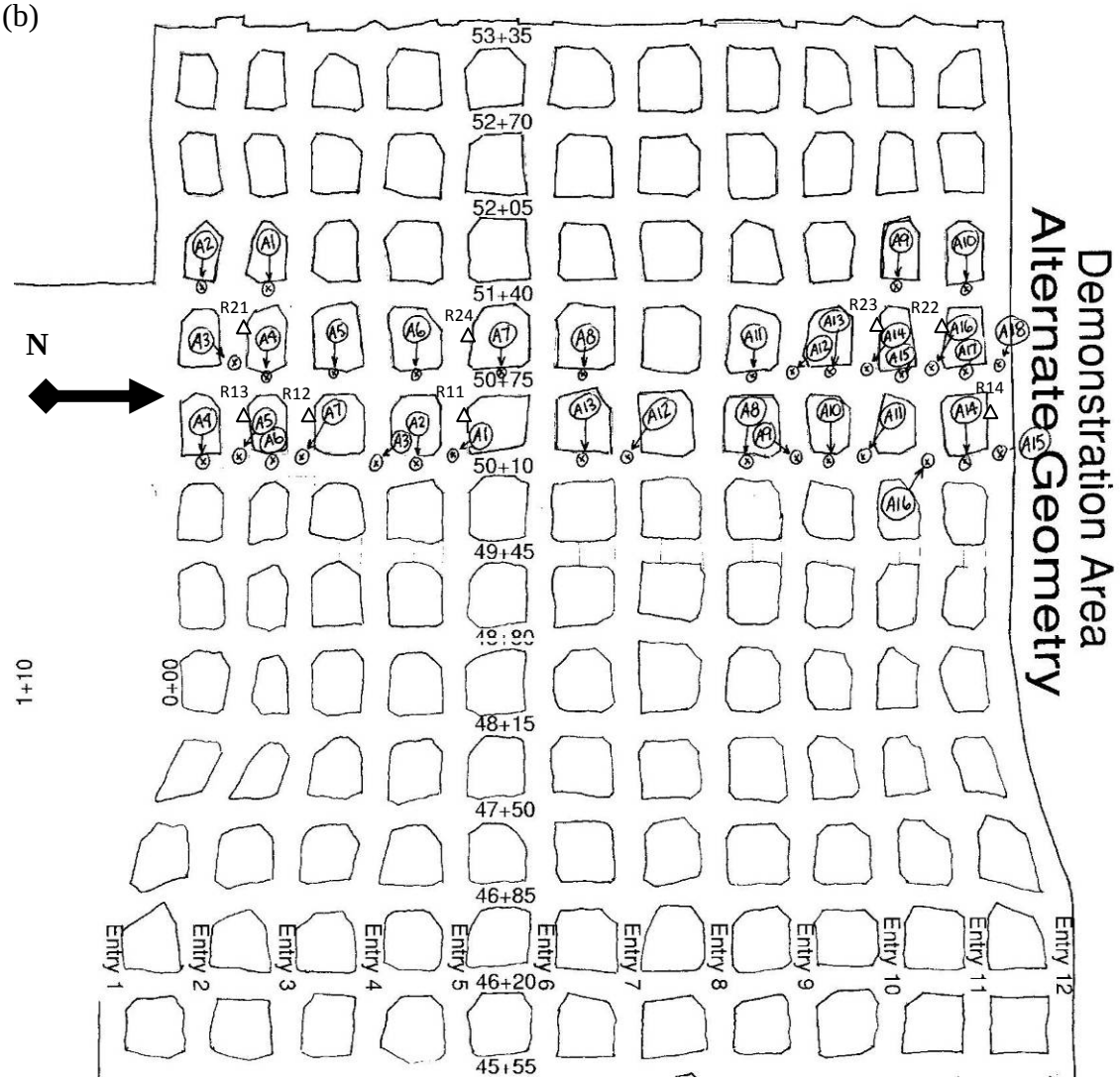

Figure 14. (a) CMG and (b) AMG demonstration areas at an Illinois Mine. Circled points represent locations of installed convergence monitoring stations and the triangle markings represent strain-rosette installation locations.

Geotechnical Monitoring in the Conventional and Alternate Mining Geometry Areas (Tasks 1.1 and 1.3)

Convergence Monitoring

Summary plots of the convergence measurements are presented in Figure 15. The average convergence measurement data is presented in Table 7. The points represented in Figure 15 are nearly equally spaced and span across the panel from left to right. Some points are also located at the intersections and they should experience higher convergence. The data was evaluated by plotting the points as a function of distance from the panel center. This analysis however did not add much to the understanding. The data presented in Figure 15 provide a better visual representation.

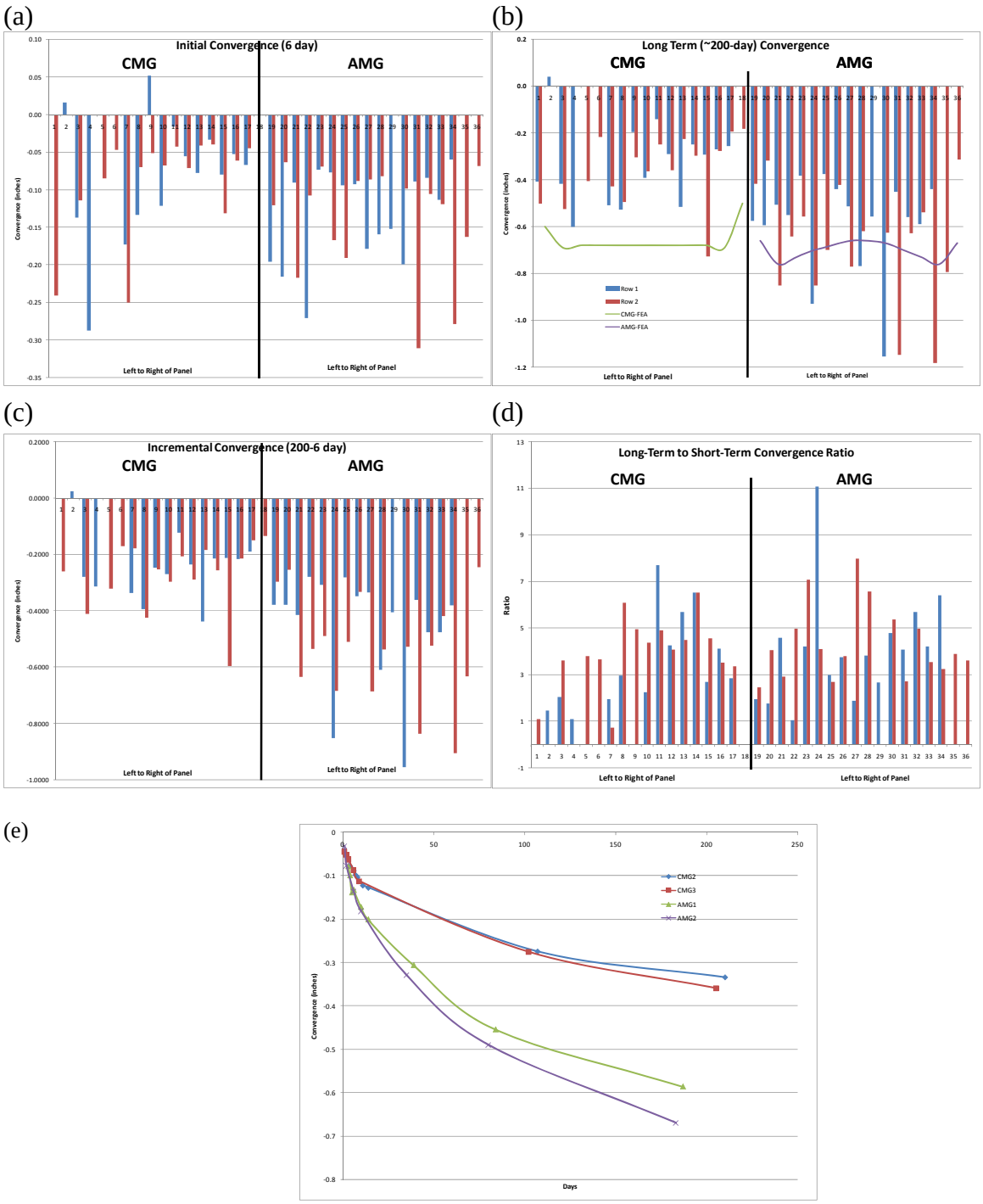

Figure 15. (a) Initial convergence (6-days after installation of points), (b) Long-term convergence (200-days after installation), (c) Incremental convergence (between 6 and 200 days), (d) Long-term to initial-convergence ratio, and, (e) Convergence deceleration curve, in the CMG and AMG represented as 18 points spread out roughly equally along the panel from left to right. Separate results for two rows of convergence monitoring stations are provided. FEA results of expected convergence are indicated in (b).

Table 7. Convergence measurement summary.

Geometry/Row	Initial Convergence (6-day), inch	Long-term Convergence (200-day), inch	Incremental Convergence (200 minus 6 day), inch	Convergence Ratio (200 day /6 day)
CMG1	0.0830	0.3340	0.2458	3.50
CMG2	0.0902	0.3586	0.2711	3.98
All CMG	**0.0867**	**0.3467**	**0.2593**	**3.75**
AMG1	0.1339	0.5858	0.4519	4.05
AMG2	0.1372	0.6688	0.5316	4.34
All AMG	**0.1356**	**0.6285**	**0.4929**	**4.20**

Figure 15 (a) represents the initial convergence measured 6-days after installation of each row of points. The average convergence in CMG and AMG was 0.0867 of an inch and 0.1356 of an inch, respectively. The long-term (200-day) convergence shown in Figure 15 (b) was 0.3467 of an inch and 0.6285 of an inch for CMG and AMG, with the coefficient of variation calculated as 45.3% and 36.6%. The lower coefficient of variation indicates that the variation in convergence across the panel was less for AMG as compared to CMG. This would be expected by design in AMG since more uniform convergence is targeted to improve roof stability.

The short-term (6-day) and long-term (200-day) convergence in AMG were about 80% higher than the CMG indicating possible bed separation, weaker coal or weaker floor in AMG. These results were due to weaker floor conditions in AMG and this was verified through plate loading tests described in a later section. The left side of the panel in CMG also showed higher convergence as compared to the right side. In the AMG the reverse was observed. Authors think that a band of weak floor strata may have been present running from the south-east to north-west in the panel as mining transitioned from CMG to AMG (Figure 16).

To further evaluate convergence behavior in the CMG and AMG, values were obtained from the Phase2 FEA model. These values are plotted along with the field convergence measurements in Figure 15 (b). The plot indicates that the convergence predicted by FEA for both the CMG and AMG is similar in magnitude. However, actual measurements in the demonstration area indicated a higher convergence in AMG as discussed earlier. This difference is again attributed to the presence of weaker floor in the demonstration area.

Rib Stress Measurements

Monitoring of rib strain-rosette points was also conducted. The ratio of the change in distance of vertical, horizontal and diagonal lines to the original distances provided the strains in the 0, 45 and 90 degree directions. These were used to calculate normal and shear stresses. However, more careful analysis by computing the Poisson's ratio indicated values which were well in excess of what would be expected from a continuum.

The reason for this was believed to be motions of the rosette points away from the plane of installation. A more realistic estimate of incremental rib stresses was thus obtained by utilizing the displacements in the vertical direction in conjunction with the elastic modulus of the coal pillar. The results are presented in Table 8. The data indicates the both CMG and AMG encountered low and similar incremental pillar stresses.

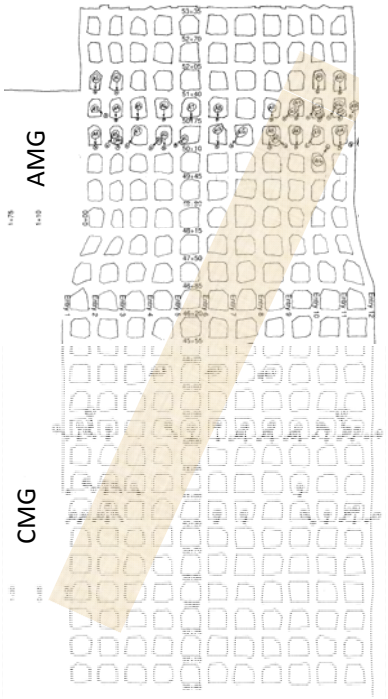

Figure 16. Hypothesized band of weak floor (represented by the shaded area) based on plate load test data collected in the CMG and AMG areas of the demonstration panel.

Additional Post-Demonstration Geotechnical Monitoring Related Studies (Task 1.3)

During a periodic monitoring and measurement visit six (6) months after demonstration, the project staff members observed a small localized area in the AMG section where a moderate amount of rib rash and a very small degree of floor heave was observed. This area is shown in Figure 14 (b) near point A14, which is on the right side of the panel. There was a consensus among project team members that the observed problems were not related to the AMG. In an effort to scientifically study this problem, plate load tests were conducted in the CMG (Location 41+65 Entry 5) and AMG (Locations 50+10 Entry 4 and Entry 9) shown in Figure 14. Floor samples for moisture content determinations were also collected. At the CMG location, floor moisture content was determined to be 9%. In the left and right portions of the AMG, the floor moisture contents were 7% and 11%. The floor strength as determined from the plate load tests was 875 psi in the CMG area, 531 psi in the right section of the AMG area and greater than 969 psi (failure did not occur) in the left section of the AMG. The 969 psi value was obtained for plate loading test on floor strata approximately 2.5 feet below the coal seam. The miner was cutting the floor in that area. Thus, the 969 psi value represents the strength of shaley limestone

rather than claystone immediately below the coal seam. The plate load test stress-displacement plot is shown in Figure 17. Hence, the results of the plate loading tests indicated that the floor was indeed significantly weaker on the right side of the AMG section. This result explained the observed localized area of rib stress and minor floor heave in this area. The weak floor was also corroborated by the higher convergence measured in this area.

Table 8. Incremental rib stresses calculated from rib rosette measurements. Points 1-5 are at the indicated locations in Figure 14. Compression is negative.

Geometry/Row/Point	Incremental Rib Stress (σ_{xx}) in the vertical direction (psi)
	σ_{xx}
CMG	
1	-1521
2	-197
3	-351
4	-261
5	-153
AMG-Row1	
1	-38
2	-138
3	-174
4	-257
AMG-Row 2	
1	-581
2	-1086
3	-56
4	-348

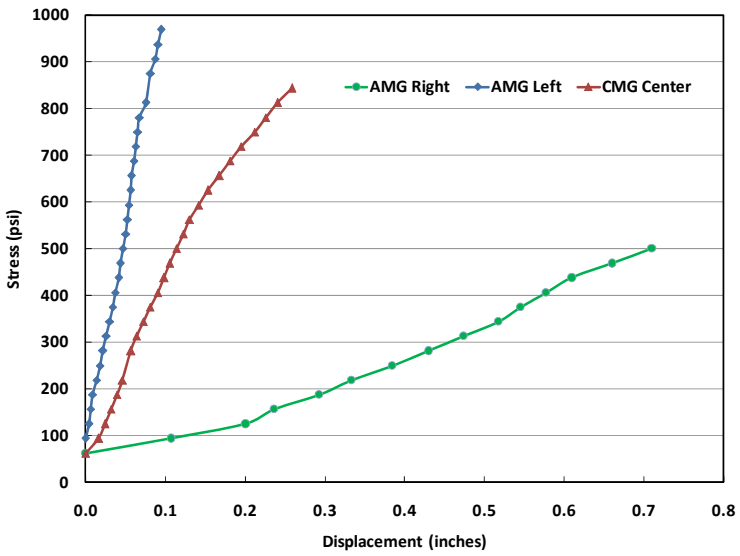

Figure 17. Plate load tests in the CMG and AMG.

Productivity Analyses (Tasks 1.1 and 1.2)

Underground coal mining involves repetitive elemental tasks often referred to as cycles. Productivity improvements involve minimizing cycle times and eliminating non-productive delays in those cycles. Typically, the maximum allowable cut depth in room-and pillar mines is 40 feet. Since the solid pillar size in CMG is 45 ft, two cuts are required to hole through every cross-cut given the uniform pillar size throughout the section and at least one of those cuts is a short one, which reduces productivity. Also reduced productivity occurs near the panel edges where wider than needed pillars mean longer haulage distances and longer cycle times. The continuous miner power cable has limited reach and reaching the end of the panels may sometimes require shifting of the cable slack. Apart from being a non-productive delay, it may also restrict movement of other equipment and decrease equipment utilization. Since AMG involves variable size pillars, it is possible to design the geometry so that there are at least some cross-cuts that can be holed through in a single cut. This has the potential to significantly increase productivity.

To compare the productivity and related cost benefits resulting from AMG, three different CMGs and five different AMGs were modeled using the SIU-Suboleski Production (SSP) Model (Chugh, et. al., 2005). The baseline CMG model using 13 entries mined straight was calibrated with data collected in the sub-mains, which involved mining 12 entries straight. The collected data included time studies conducted by the project team as well as earlier data collected by the mine's process improvement team. Even though the CMG and AMG demonstration involved 12 entries, production modeling emphasized an odd number of entries (13 and 15) as this is more typical and widely employed in super-sections.

The modeled sub-mains utilized a split air ventilation system in a super-section. It produced about 3,200 raw tons/shift, working 213 days/year, and 3 shifts/day. The panel used two Joy 12 CM continuous miners, four (4) battery ram cars (9-10 ton capacity) and three (3) double-boom roof bolters. The analysis assumed identical production and equipment characteristics for all other modeled geometries. The following geometries were modeled and compared using the SSP model. The unique pillar arrangements in the specific AMGs are presented in Table 9. All the AMGs were developed and modeled after discussion with the mine operations staff.

1. SREG13-65: This geometry is a 13-entry system with twelve pillars on 65-ft centers. The baseline CMG which was utilized in the sub-mains was similar to this geometry with the exception that it involved 12 entries and 11 pillars as shown in Figure 10 (b). The demonstrated geometry is somewhat atypical and hence, for a more generalized comparison, production modeling was based on a 13-entry system and compared with alternate geometries also mining 13 entries.
2. SREG13-65-F: This geometry was identical to SREG13-65 with the exception that fender cuts were made into the barrier pillars. Making fender cuts is a popular practice as it increases extraction ratio and reduces costs as the fender cuts can be left unbolted. However, panel stability is somewhat compromised.

3. RREG595-F: This geometry involves mining 9 entries straight and developing sets of rooms which are five pillars deep on either side of the panel. The area in the rooms is extensively fendered as shown in Figure 18. This geometry is also a popular conventional geometry.

Table 9. Pillar sizes in five comparative geometries modeled using SSP model. 1-14 represent pillars with the pillar width (c-c) indicated below in feet. The pillar lengths are either 65 or 60-feet c-c as indicated in the first column. REG geometry is the CMG while the ALT geometries are the AMGs.

Pillar Sizes

	1	2	3	4	5	6	7	8	9	10	11	12	13	14
SREG13-65 65-ft centers in direction of advance	65	65	65	65	65	65	65	65	65	65	65	65		
SALT13-65 65-ft centers in direction of advance	50	50	50	60	65	65	65	65	60	50	50	50		
SALT13-60 60-ft centers in direction of advance	50	50	50	60	65	65	65	65	60	50	50	50		
SALT15-65 65-ft centers in direction of advance	50	50	50	55	60	65	65	65	65	60	55	50	50	50
SALT15-60 60-ft centers in direction of advance	50	50	50	55	60	65	65	65	65	60	55	50	50	50

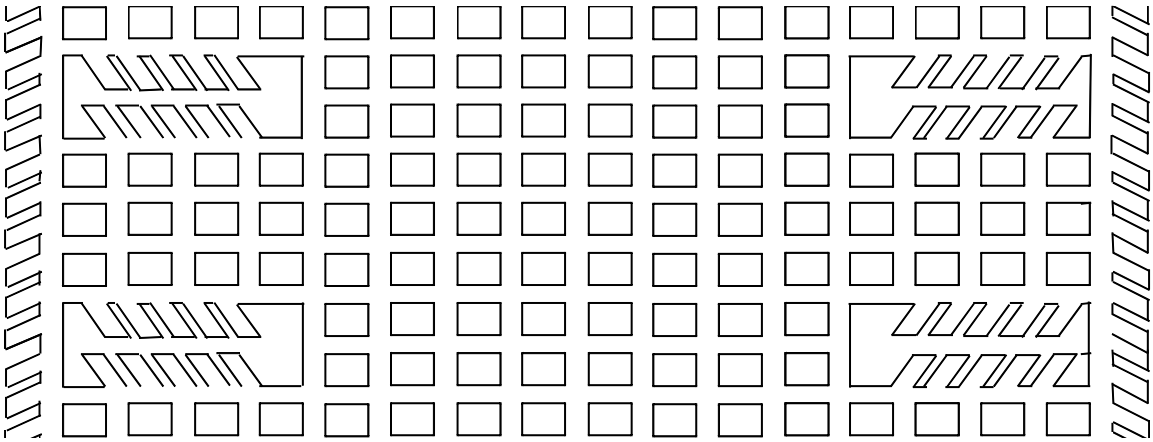

Figure 18. RREG595-F CMG showing the nine central entries mined straight and sets of rooms five pillars deep on either side.

4. SALT13-60: This was an alternate geometry involving variable size pillars on 60-ft centers in the direction of advance.
5. SALT13-65: This AMG is similar to SALT13-60 with the exception that the pillars are on 65-ft centers in the direction of advance. This was the AMG demonstrated at the mine (in a 12 entry configuration) and compared against the CMG described by SREG13-65.
6. SALT13-60-F: This geometry was identical to SALT13-60 with the exception of using fender cuts. This geometry was a comparable AMG to the SREG13-65-F CMG.
7. SALT15-65: This was an alternate geometry that was developed as an alternative to avoid fender cuts. Two additional entries on either side were incorporated as a substitute for fender cuts. There was an option in this geometry to leave portions of these peripheral entries unbolted. The additional entries also served the purpose of restoring the initial panel footprint which would be reduced with the

use of smaller size pillars.

8. SALT15-60: This geometry was the same as SALT15-65 but for the 60-ft center entries in the direction of advance.

Development of Unbiased Cut-Sequences for Comparison

Since production is dependent on the utilized cut sequence, a significant effort was devoted towards developing rules for cut-sequencing and the cut sequences themselves, for each geometry such that the resulting sequences would be unbiased and comparable. The following cut-sequencing rules were developed and followed.

1. Cut rooms (cross-cuts) with the air - When connecting two entries with a cross-cut, mining in the direction that is co-current with the air flow reduces the respirable dust levels at the miner and ram car operator's positions. Once a cross-cut is "holed" the intake or fresh air flows over the ram car and miner operators carrying the dust away from them. Mining into the air flow results in the dust being carried directly over these operators.
2. Cut sequences should repeat every cross-cut, if possible - Cut sequences that allow for the entire sequence to repeat every cross-cut usually reduce the length of travel for the continuous miner from place to place, keep the advancement of entries even allowing for better ventilation of the face area, improve ram car efficiency by keeping the length of travel to the belt feeder at a minimum, and allow for improved scheduling of belt and power advancements.
3. Always mine perimeter cuts in pairs - When making perimeter cuts and following a cut sequence that repeats itself each cross-cut, mining the two perimeter cuts that are available during each cross-cut of advancement in sequence improves mining efficiency. Making both of these cuts in succession reduces move time for the continuous miner.
4. Start cross-cuts head-on rather than turning where possible - Mining cross-cuts by starting the cut "head on" into the cross-cut (starting perpendicular to the coal block) is more efficient as compared to "turning" the cross-cut (starting parallel to the coal block and turning 90 degrees to the right or left). Turning a cross-cut cause the miner cutting drum to incrementally contact the coal face thus increasing load times, while mining head-on into the coal face allows for the entire miner cutting drum to immediately contact the face. Hitting the cross-cut head-on also allows the miner and ram-car operators to remain in the last open cross-cut where dust levels are lower as a result of the higher volume of available air at that location.
5. Leave one cut spacing between the miner and the roof bolter when the cuts are of equal length - The cutting sequence should allow the continuous miner to move into a cut that was not sequentially mined previous to the present cut when mining cuts of equal length. In most cases where cuts are of equal length, the roof bolter can support a cut faster than the continuous miner can mine it. Roof conditions, re-supplying the bolter and mechanical problems can reduce roof bolting speeds and therefore a "cushion" of at least one cut is advisable.
6. In cross-cuts requiring two cuts to hole through, follow the second cut with

another cut that does not require moving cable, if possible - When mining through a cross-cut, backing up into the entry and mining ahead allows for minimal cable movement. This reduces move times and substantially increases production.

7. Avoid both miners being in the middle or side of entries of the panel at the same time - Keeping the miners at the approximate same distance apart (same number of entries) eliminates both miners experiencing long ram car cycle times simultaneously. When one miner is in the middle of the panel, the other should be at or near the perimeter and should avoid both being in the middle of the panel at the same time. This spacing allows ram cars routes to not overlap and reduces dust exposure for the downwind miner or bolter.
8. Advance ventilation (complete cross-cuts) on the left side first - When using one side of the panel (right side) as the intake and the left side as the return, advancing the stoppings on the left side improves the efficiency of the ventilation system. This keeps the air moving toward the face and reduces the dust levels in the middle or neutral areas of the panel where ram cars and other equipment travel.

The final cut sequences were presented to mine professionals before they were used in production modeling. The final cut sequences for five of the modeled geometries are presented in Figure 19 as an example. The results of the production model simulations are presented in Table 10. The simulation results indicate that all of the AMGs outperform the CMGs in terms of higher productivity, lower cost and higher extraction ratio. When comparing an unfendered geometry using the same number of entries, a productivity increase of 5-6% was projected at a corresponding cost reduction of 3.0%.

Table 10. SSP production model results summary comparing the CMGs and AMGs. RTPUS – raw tons per unit shift. Production Cost is the Face production cost and includes all costs for mining and transporting the coal up to the sub-main belt. Extraction ratio reported here includes the coal extracted in fender cuts and does not consider the barrier pillar.

		Extraction Ratio (%)	Production RTPUS	Production Cost $/ton
CMG	**SREG13-65**	53.3%	3159	$7.66
CMG	**SREG13-65-F**	59.7%	3169	$7.48
CMG	**RREG595-65**	55.1%	3239	$7.34
AMG	**SALT13-65**	55.9%	3316	$7.43
AMG	**SALT13-60**	57.5%	3352	$7.43
AMG	**SALT15-65**	55.9%	3366	$7.29
AMG	**SALT15-60**	57.5%	3384	$7.26
AMG	**SALT13-60-F**	65.2%	3421	$7.17

(a)

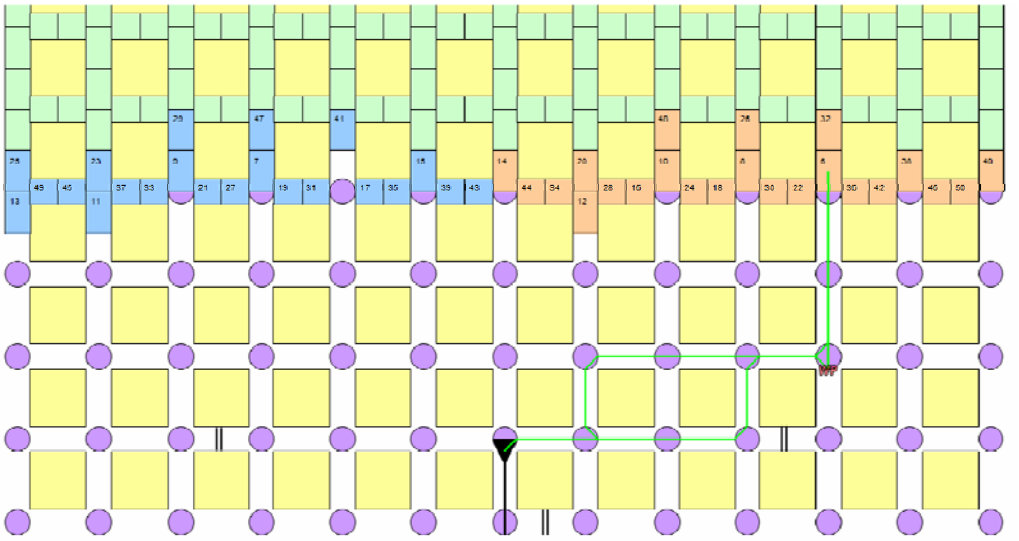

(b)

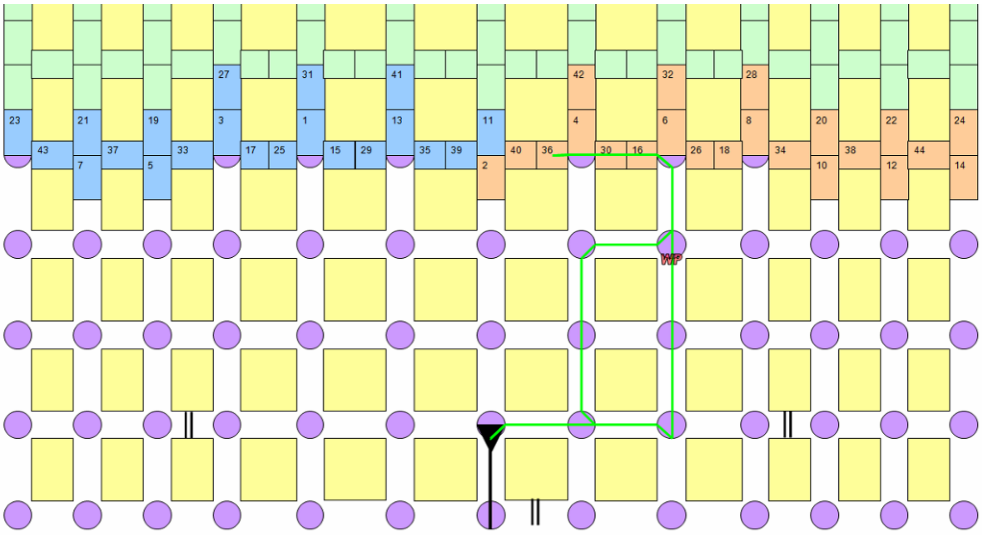

(c)

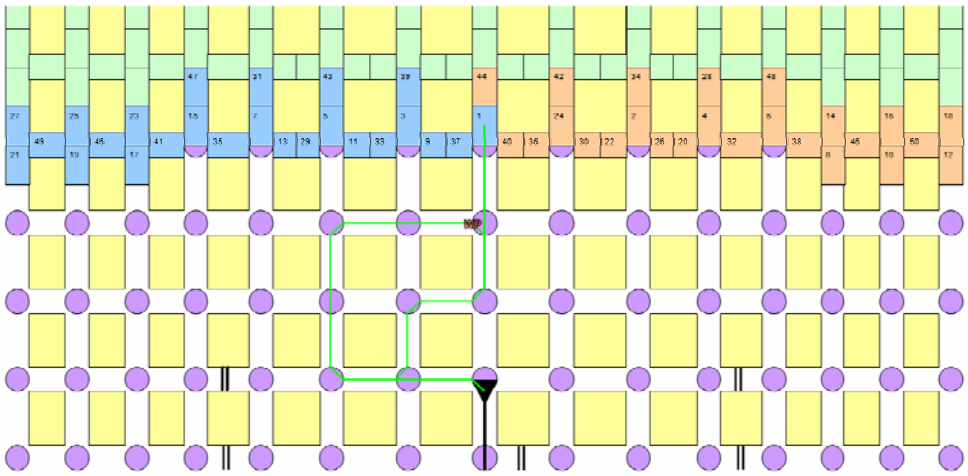

Figure 19. Cut Sequence utilized in SSP modeling of (a) 13-entry CMG (SREG13-65), (b) 13-entry AMG (SALT13-65 and SALT 13-60), and, (c) 15-entry AMG (SALT15-65 and SALT15-60).

The extraction ratio increase was projected to be 2.6-4.2%. When comparing CMGs and AMGs utilizing fender cuts, a 7.9% increase in productivity at a cost reduction of 4.1% and an increased extraction ratio of 5.5% was predicted. When comparing a 13-entry CMG with fender cuts to a 15-entry AMG without fender cuts, a productivity improvement of 6.8% at a cost reduction of 2.9% is projected, although the extraction ratio in this comparison declines. However, considering the possibility that the mining geometry without fender cuts is more stable and does not involve fender cuts into the barrier pillar, a smaller barrier pillar could be used. This will enhance the overall extraction ratio. The superior productivity and related cost reduction with the AMG were analyzed and were found to be primarily driven by the ability to mine cross-cuts between the outer entries with a single-cut, blow-through as mentioned above.

In addition to production and cost analysis of the different geometries, the delays in each cut in each of the modeled geometries were also analyzed. Wait times in a mining system can indicate both loss of productive time as well as overcapacity of the system. In a CM-batch haulage system, overcapacity is indicated by haulage cars waiting on the miner while loss of production time is indicated by the miner waiting on cars (Chugh et. al., 2005). Frequency distributions of wait times were plotted for different geometries from modeling results. Positive wait times indicate a wait on car (miner waits on cars) while a negative wait time indicates a wait on miner (car waits on the miner). Figure 20 shows the histogram of wait times for different geometries. Analysis of the histogram shows that in almost all of the cases the wait times are negative which indicate the batch haulage units are waiting on the miner. Comparing the three histograms, it is observed that AMG #1 (Figure 10 (b)) has more bias towards the zero wait time. Thus AMG #1 is a better matched system as compared to the other geometries and should therefore provide close to maximum achievable production.

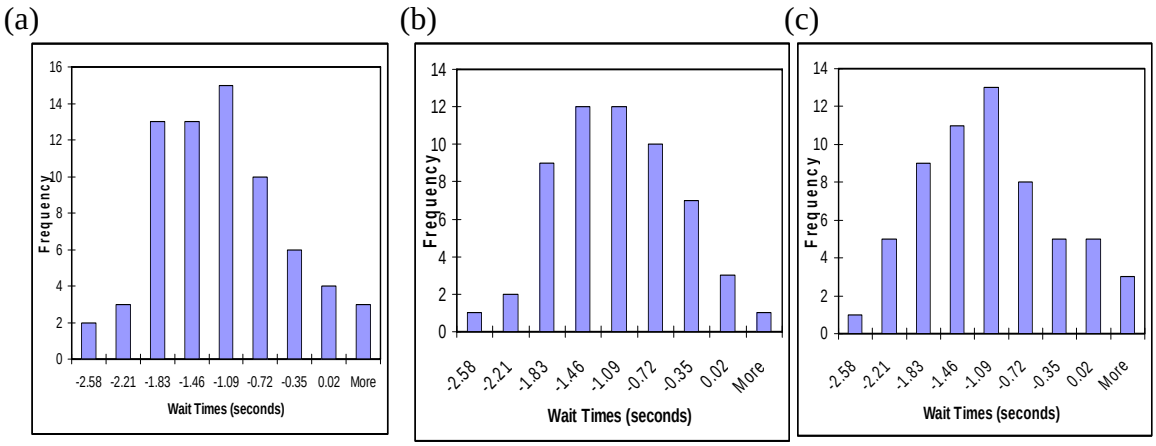

Figure 20. Histogram of wait times for different geometries (a) CMG, (b) AMG#1 (represented by Figure 10 (b)), and (c) AMG#2 (represented by Figure 10 (c)).

As discussed earlier, actual production numbers during the AMG demonstration were slightly lower than those during the CMG. The reason for this difference was that a sub-optimal cut sequence was followed during the AMG mining. Instead of making single-

cut blow-through for cross-cuts in the smaller pillars, the cuts were made by turning from both left and right. This practice is worse than the conventional practice of turning and blowing through in two cuts. The reason for selecting this cut sequence during mining is unknown. Authors think that the reason could be that the miners were not familiar with mining in the AMG.

OSD Measurements (Task 1.4)

To determine the impact of AMG on OSD, a roof and floor mined thickness measurement program was conducted approximately seven (7) months after demonstration. It was thought that OSD might be reduced due to improved stability of mine workings. Measurements were conducted across four cross-cuts each in the CMG and AMG areas. Mining height, along with mined roof and floor thickness measurements were taken in the entries, cross cuts and on the four faces of all the pillars. The developed data was analyzed statistically. The sampling locations are indicated in Figure 21. The measurement results are presented in Table 11. The almost identical seam height measurements in both the geometries is indicative of the measurement accuracy since the seam height would not be expected to change significantly over a distance of four cross-cuts. The very similar measurements of the mined floor thickness in the CMG and AMG, both in terms of the average and standard deviation are indicative of similar mining practice followed in the two geometries. The most interesting result relates to the roof thickness where an almost 50% reduction in the mined roof thickness is indicated. The result is statistically significant at a level higher than 99.9%. As would be expected, the total mined height is also lower for the AMG. Thus, the results indicate that there was reduced roof dilution in the AMG. Benefits arising from lower roof dilution could involve lower equipment maintenance, lower cost, increased preparation plant recovery and efficiency and better product quality.

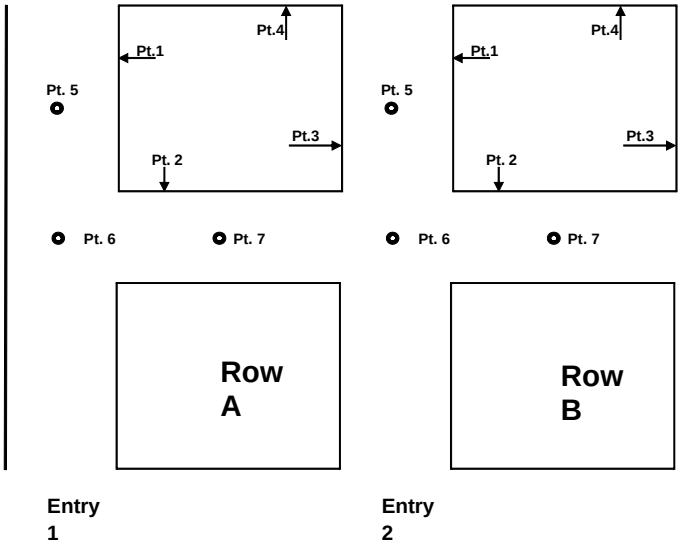

Figure 21. OSD measurement locations in the CMG and AMG. Roof, seam and floor heights were measured for points 1-4. Only total mining height was measured at points 5-7.

Table 11. OSD measurement results summary. S.D – Standard Deviation, N – Number of measurements.

Parameter	Conventional Mining Geometry (inches)				Alternate Mining Geometry (inches)			
	Mining Height	Seam Height	Mined Roof	Mined Floor	Mining Height	Seam Height	Mined Roof	Mined Floor
Average	82.5	73.3	4.3	4.1	81.2	73.1	2.4	4.3
S.D	4.4	2.5	4.1	2.9	3.9	2.5	2.0	3.1
N	275	154	155	155	279	158	158	158

Task 2: Optimizing Cut Sequences

The approach behind developing an optimum cut sequence focuses on the following key points:

- Completing cross-cuts in a timely fashion is critical for establishing and maintaining adequate face ventilation, minimizing change-out distances, and ensuring uniform face advance across a miner section.
- Within acceptable rock mechanics parameters, smaller entry spacing (the distance between centerlines of adjacent entries) and larger cross-cut spacing (the distance between centerlines of adjacent cross-cuts) minimizes the amount of time spent mining cross-cuts, which is generally the slowest mining.
- The least productive cuts in a cut cycle are those that must be "turned" at an angle from the general direction of mining in main entries.
- Cuts with longer change-out distances are more difficult to ventilate.
- Mining cross-cuts in the direction of ventilation air flow on a mining section reduces occurrences of cross-cuts being "holed through" (completed) against the ventilating current and all of the dust surrounding the continuous miner head blowing into the area occupied by the miner operator.

Dynamic programming has been used in many different mining scenarios to solve the problem of scheduling optimized mining sequences. A brief explanation of dynamic programming as an optimization algorithm for cut sequencing was provided in the first phase final report, (Chugh et. al., 2006). The very basic optimal value function described in that report has been further refined to the following:

Minimize CCT

where, CCT = {BF * VF * [COD + (TD * CHF)]}
and, CCT = cut cycle time
BF = bolting factor or constraint
VF = ventilation factor or constraint
COD = change-out distance
TD = miner tram distance from previous cut
CHF = cable handling factor or constraint.

Change-out distance and tram distance are self explanatory. To utilize the dynamic programming algorithm in this phase of the project, values for the three factors in the optimal value function were selected based on general mining practices and experience. Those values and the reasoning behind them are described below. Research is ongoing to develop factor values that are more grounded in scientific principles while still providing realistic results.

Bolting Factor - To be considered feasible, a cut must be accessible through previously mined cuts. However, complete accessibility requires previously mined cuts to be bolted. Thus, the bolting factor is used to render the most recently mined cut an impossible candidate for the next cut. The bolting factor can also be used to maintain a buffer between mining and bolting functions requiring the continuous miner to make one, two or even more cuts in other entries before returning to an entry to make the next cut. At the demonstration mine, time study observations indicated that bolting was not a constraint, but management desired two cuts be mined between adjacent cuts in a given entry. Thus, the bolting factors used in the optimal value function are as follows:

BF = 10	if available cut is bounded by previous cut just made
BF = 4	if available cut is bounded by cut made 1 cut previous
BF = 2	if available cut is bounded by cut made 2 cuts previous
BF = 1	if available cut is bounded by cut made 3 or more cuts previous
BF = 5	if available cut is bounded by cross-cut mined on previous cut

Since bolting factor is a multiplier in the recursion formula, the higher factors of 10, 5 and 4 effectively prevent certain cuts from being selected. This is primarily a safety measure to keep the miner operator from working near unsupported top.

Ventilation Factor - Cross-cuts can be the most difficult cuts in the cut sequence cycle due to long and awkward change-outs for the haulage equipment and the inefficiencies of "turning" a cross-cut. However, keeping cross-cuts caught up with main entry advance is critical in maintaining adequate ventilation and providing haulage equipment access to change-out points that are as close to the face as possible. The ventilation factor is used to make feasible cuts that would begin or complete a cross-cut preferable to other cuts. It is also used to direct that cross-cuts be mined in the direction of ventilation air flow at the face ("with the air") and that the continuous miner is positioned so that the scrubber configuration is able to utilize the direction of air flow and does not have to work against it. Starting cross-cuts "head on" is made preferable to "turning" a cross-cut. The ventilation factor capitalizes on one of the advantages of alternate geometry in that cross-cuts between outside entries can be started and completed in the same cut. Ventilation factors used in the optimal value function for the alternate geometry of the demonstration area are as follows:

VF = 2	if available cut is in an entry that is mined deep enough to turn a cross-cut
VF = 1	if available cut is in an entry that is not mined deep enough to turn a cross-cut
VF = 0.5	if available cut is in an entry that needs to be driven up to turn a cross-cut

VF = 0.75 if available cut starts a cross-cut and it can be mined “head on”
VF = 0.5 if available cut completes a cross-cut and can be “holed through” “with the air”
VF = 1.5 if available cut starts a cross-cut and it has to be “turned”
VF = 1.25 if available cut completes a cross-cut but is “holed through” “against the air”
VF = 2 if available cut starts a cross-cut that has to be turned on scrubber side

The ventilation factor is also a multiplier in the recursion formula. Thus, a ventilation factor greater than 1 will inhibit a cut from being selected while a ventilation factor less than 1 will encourage selection of that cut.

Cable Handling Factor - As the miner moves from cut to cut, it is either pulling slack cable or picking it up. Little time and effort is involved in pulling cable whereas considerable time and effort is required to handle the miner cable when slack has to be picked up or hung. The cable handling factor promotes sequencing of cuts such that the number of times that slack cable has to be picked up is minimized and when it is done, the miner cable is positioned so that the miner is able to make a number of cuts without rehandling the cable. The cable handling factor can be used to give preference to “double cutting” or making two cuts from the same entry such as a cut in a straight followed by “turning” a cross-cut. Cable handling factors used in the cut sequence optimization algorithm are as follows:

CHF = 0.8 if making a second cut from the same entry (“double cutting”)
CHF = 1 if pulling slack and moving 1 entry away
CHF = 1.25 if pulling slack and moving more than 1 entry
CHF = 1.5 if pulling slack and hanging cable
CHF = 1.8 if picking up slack and moving 2 entries or less
CHF = 2 if picking up slack, moving 2 entries or less and hanging cable
CHF = 2.15 if picking up slack and moving more than 2 entries
CHF = 2.25 if picking up slack, moving more than 2 entries and hanging cable

Tram distance has a direct impact on how much time the miner spends mining coal. The cable handling factor is used to enhance that impact in the recursion relationship. A cable handling factor greater than 1 makes cuts requiring long tram distances less likely to be selected while a cable handling factor less than 1 reduces the impact of tram distance in the recursion formula.

The alternate geometry demonstration area was a submain with 12 entries mined by two continuous miners as a supersection. Figure 22 shows a 2-cross-cut cutting cycle for the left side of the section. The right side is a mirror image with the line of symmetry being the line between cuts 32 and 33. The power center (PC) for the left side is located in the #5 entry (numbering from the left side). Following a belt and power move the continuous miner will be positioned in the #5 entry between the PC and the face.

When the entries are driven and the section is squared off with cross-cuts, each entry face

is typically advanced beyond the cross-cuts to some degree. For the purposes of this analysis, 25 feet of advance beyond the last open cross-cut centerline is used. Cross-cuts were on 65-foot centers in the demonstration area so a mining depth of 32.5 feet was used for main entry cuts. A cut depth of 15 feet was used for cross-cuts "turned" from main entries. Cross-cuts mined "head on" were limited to a depth of 35 feet.

Results from the dynamic programming optimization routine for this scenario are provided in the appendix in tabular form. In using this recursive approach, a value is determined for each possible cut by way of the optimal value function and the cut with the smallest value is selected as the optimum cut to make next. The model suggests the cut sequence shown in Figure 23. The recommended cut sequence is essentially repetitive for each cross-cut that the section advances. It should be noted that cuts 32 and 33 are shared between the two miners. Also, when the section is squared off prior to a belt and power move, #4 and #5 entries will be advanced one cut beyond the other entries.

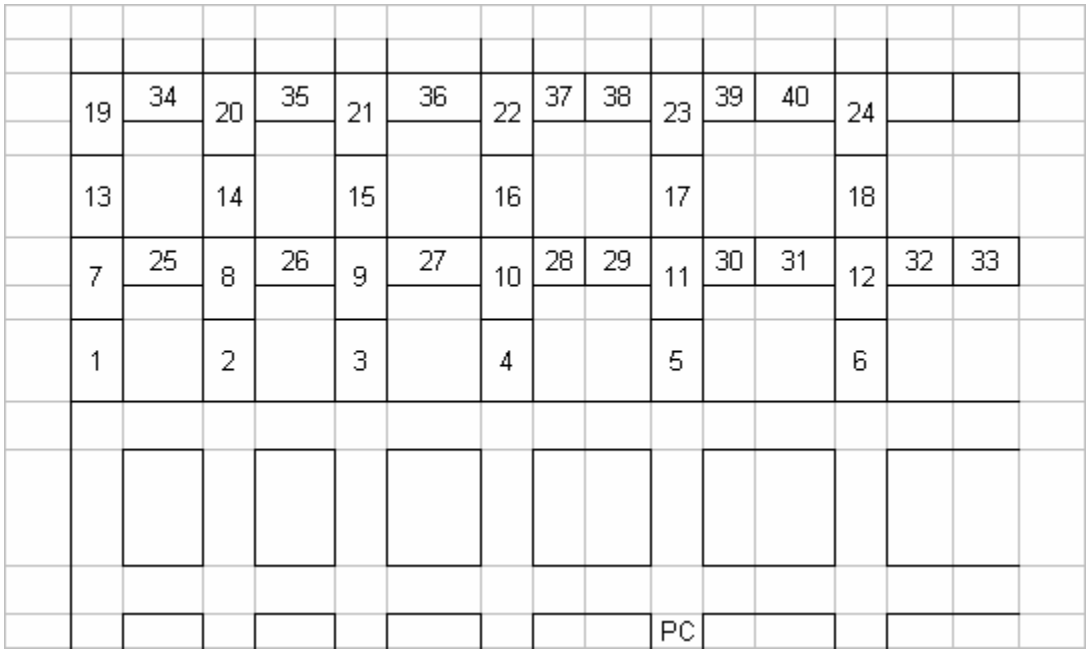

Figure 22. Individual cuts in a two-cross-cut cycle for left-side miner in demonstration area.

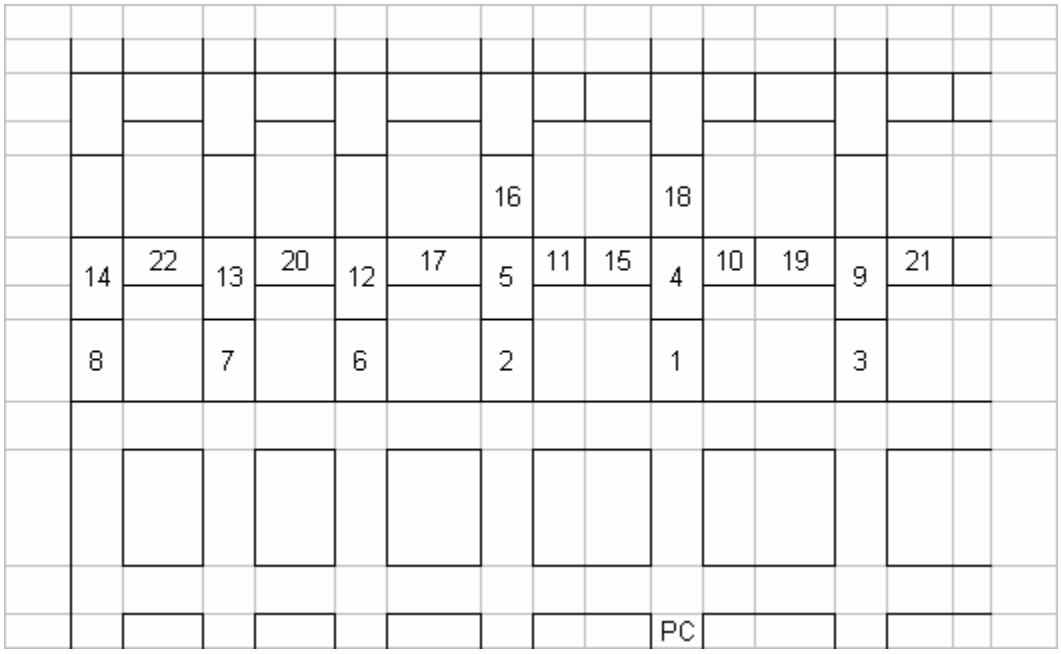

Figure 23. Cut sequence suggested by iterations of the dynamic programming model.

CONCLUSIONS AND RECOMMENDATIONS

The following conclusions were developed from the design and demonstration of an alternate mining geometry at an Illinois mine in this project. The alternate mining geometry concept utilized unequal pillar sizes with larger pillars around the center and smaller pillars around the edges of a mining section to increase extraction ratio, improve panel stability and enhance productivity.

1. The demonstrated alternate geometry increased extraction ratio by 3.2%. Authors believe the extraction ratio could have been increased an additional 1-2% without negatively impacting panel stability.
2. Production modeling studies indicate that about 7% increase in productivity with estimated 4% reduction in production cost can be achieved with the demonstrated alternate geometry. This is due to the ability to mine cross-cuts between the outer entries with a single cut blow-through which reduces the number of miner moves.
3. Geotechnical monitoring of the alternate geometry indicated a more uniform but higher convergence compared to the conventional geometry. The higher observed convergence appears to be related to weak floor conditions in the AMG area. FEA results on convergence indicate a very similar total convergence in both AMG and CMG.
4. A 50% reduction in OSD from the roof was documented in the alternate geometry. This is believed to be a result of improved roof stability.
5. The localized rib stress and floor heave observations in the alternate geometry section are not related to mining geometry but due to a band of weak floor running through the AMG mining area.

6. The results of current and previous demonstrations of AMG in Illinois indicate that the mining industry can increase extraction ratio by 3-5% and increase productivity by 5-7% through use of AMG in room-and-pillar mining.
7. Finite element analyses indicate that alternate mining geometry provides improved ground control as compared to conventional geometry currently in use.
8. FSF values calculated using Vesic-Speck and FEA approaches are very similar indicating that equations for computing bearing capacity of foundations over non-homogeneous layered strata are analytically valid.

Authors have developed the following recommendations.

1. The two field demonstrations in Illinois have concluded that the AMG concepts are technically sound and have the potential to increase both extraction ratio and production rates while maintaining geotechnical stability of mine workings.
2. Industry should consider and adopt this mining practice based on appropriate geotechnical investigations of the areas where it will be adopted. Longer-term geotechnical monitoring of the mining areas should be an integral part of this adoption to further improve confidence in the concepts for both mining companies and regulatory agencies.

ACNOWLEDGEMENTS

In addition to the funding support provided by Illinois Clean Coal Institute (ICCI) and the Department of Commerce and Economic Opportunity, the authors also acknowledge the research assistance support provided by the Coal Research Center at SIUC. The authors also appreciate the support of the ICCI project manager, Dr. Ronald Carty, and the participation of Mr. Joseph Hirschi, ICCI, in the productivity analysis and cut sequence optimization tasks of this project. The outstanding support provided by the mine and corporate level professionals of the participating coal company is also appreciated and has been a major factor in the success of this project.

REFERENCES

1. Chugh, Y.P. and Pytel, W. 1992a. “Design of Partial Extraction Coal Mine Layouts for Weak Floor Strata Conditions”, Information Circular 9315: 32-49, U.S. Bureau of Mines.
2. Chugh, Y.P. and Pytel, W. 1992b. “Analysis of Alternate Room-And-Pillar Mining Geometries Using the SIU PANEL.2D Model”. In Mine Systems Design and Ground Control, In Proceedings Annual Workshop, Generic Mineral Technology Center: 71-82, Moscow, Idaho.
3. Chugh, Y.P., and Pytel, W. 2004a. “Development of Alternate Room-and-Pillar Mining Geometries for Improved Extraction and Ground Control in Coal and Copper Mines”, In Proceedings of 13th Mine Planning and Equipment Selection Symposium, Wroclaw, Poland, Sep. 1-3.

4. Chugh, Y., W. Pytel, and J. Ma, 2004b, “Development and Demonstration of an Alternate Mining Geometry for Improved Ground Control in an Illinois Coal Mine”, 23rd International Conference on Ground Control in Mining, Morgantown, WV, Aug. 3-5.
5. Chugh, Y.P., Hao. 1992. “Design of Coal Pillars” SIU software.
6. Chugh, Y.P., Moharana, A., and Patwardhan, A., 2005 “Development of Simple Production Modeling Software for Continuous Miner Production System”, In Proceedings of 14th Mine Planning and Equipment Selection Symposium, Banff, Canada, Oct. 31-Nov. 3.
7. Chugh, Y.P., Pytel, W., and Ma, J.2004. “Development and Demonstration of an Alternate Mining Geometry for Improved Ground Control in an Illinois Coal Mine”, In Proceedings of 23rd International Conference on Ground Control in Mining, Morgantown, WV, USA, Aug. 3-5.
8. Chugh, Y. P., Patwardhan, A., Gurley, H., Moharana, A. and Pulliam, J., 2006, “Development and Demonstration of Alternate Room-and-Pillar Mining Geometry in Illinois”, Project No. DEV05-11, Final report to Illinois Clean Coal Institute.
9. Engineering Handbook, Chap. 3, H.F. Winterkorn, and H. Fang, eds., Van Nostrand Reinhold, New York, p. 121–147.
10. Goodman, R.E., 1980, “Introduction to Rock Mechanics” John Wiley and Sons, New York, p 355-359.
11. Holland, C.T., 1964, “The Strength of Coal Pillars” In proceedings of 6th US Symposium on Rock Mechanics, University of Missouri, Rolla, pp. 450–466.
12. Holland, C.T., 1973, “Mine Pillar Design” SME Mining Engineering Handbook, Vol. 1, Sec. 13-8, AIME, New York, pp. 97–118.
13. Pytel, W. 2003. “Rock mass - mine workings interaction model for Polish copper mine conditions”, Int. J. of Rock Mech. & Min. Sci. (40): 497-526.
14. Pytel, W. and Y. Chugh, 1991. Development of SIU Ground Mechanics Models, Final Technical Report and User’s Manual to Generic Mineral Technology Center, Mine Systems and Ground Control, 220 pp.
15. RocScience,Web-site: http://www.rocscience.com/products/rocdata/StrengthCriteria.asp. Last accessed on September 11, 2006.
16. Vesic, A.S., 1975, “Bearing Capacity of Shallow Foundations” Foundation.

DISCLAIMER STATEMENT

This report was prepared by Dr. Yoginder P. Chugh, Southern Illinois University, Carbondale with support, in part, by grants made possible by the Illinois Department of Commerce and Economic Opportunity through the Office of Coal Development and the Illinois Clean Coal Institute. Neither Dr. Yoginder P. Chugh and Southern Illinois University, Carbondale, nor any of its subcontractors, nor the Illinois Department of Commerce and Economic Opportunity, Office of Coal Development, the Illinois Clean Coal Institute, nor any person acting on behalf of either:

(A) Makes any warranty of representation, express or implied, with respect to the accuracy, completeness, or usefulness of the information contained in this report, or that the use of any information, apparatus, method, or process disclosed in this report may not infringe privately-owned rights; or

(B) Assumes any liabilities with respect to the use of, or for damages resulting from the use of, any information, apparatus, method or process disclosed in this report.

Reference herein to any specific commercial product, process, or service by trade name, trademark, manufacturer, or otherwise, does not necessarily constitute or imply its endorsement, recommendation, or favoring; nor do the views and opinions of authors expressed herein necessarily state or reflect those of the Illinois Department of Commerce and Economic Opportunity, Office of Coal Development, or the Illinois Clean Coal Institute.

Notice to Journalists and Publishers: If you borrow information from any part of this report, you must include a statement about the state of Illinois' support of the project.

APPENDIX

Dynamic Programming Model Iterations

Cuts Available for 1st cut		1	2	3	4	**5**	6						
	Bolting factor	1	1	1	1	1	1						
	Ventilation factor	1	1	1	0.5	0.5	0.5						
	Cable handling factor	1.25	1.25	1.25	1	1	1.5						
	Change-out distance	90	90	90	25	25	25						
	Tram distance	250	200	150	95	35	100						
	Recursion value	403	340	278	60	**30**	87.5						
Cuts Available for 2nd cut		1	2	3	**4**	11	6						
	Bolting factor	1	1	1	1	10	1						
	Ventilation factor	1	1	1	0.5	0.5	0.5						
	Cable handling factor	1.25	1.25	1.25	1	0.8	1.5						
	Change-out distance	90	90	90	25	58	25						
	Tram distance	298	248	198	143	0	148						
	Recursion value	462	399	337	**83.8**	288	123						
Cuts Available for 3rd cut		1	2	3	10	11	**6**						
	Bolting factor	1	1	1	10	4	1						
	Ventilation factor	1	1	1	0.5	0.5	0.5						
	Cable handling factor	1.25	1.25	1	0.8	1.8	2						
	Change-out distance	90	90	90	58	58	25						
	Tram distance	238	188	138	0	175	208						
	Recursion value	387	324	228	288	745	**220**						
Cuts Available for 4th cut		1	2	3	10	**11**	12						
	Bolting factor	1	1	1	4	2	10						
	Ventilation factor	1	1	1	0.5	0.5	0.5						
	Cable handling factor	1.25	1.25	1.25	1.25	1	0.8						
	Change-out distance	90	90	90	58	58	58						
	Tram distance	363	313	263	240	180	0						
	Recursion value	543	481	418	715	**238**	288						
Cuts Available for 5th cut		1	2	3	**10**	12	17	29	30				
	Bolting factor	1	1	1	2	4	10	10	10				
	Ventilation factor	1	1	1	0.5	0.5	2	2	1.5				
	Cable handling factor	1.25	1.25	1.25	1	2	0.8	0.8	0.8				
	Change-out distance	90	90	90	58	58	90	75	75				
	Tram distance	330	280	230	208	213	0	35	35				
	Recursion value	503	440	378	**265**	965	1800	2060	1545				
Cuts Available for 6th cut		1	2	**3**	12	16	17	27	28	29	30		
	Bolting factor	1	1	1	2	10	4	10	10	4	4		
	Ventilation factor	1	1	1	0.5	2	2	2	1.5	2	1.5		
	Cable handling factor	1.25	1.25	1	2	0.8	1.8	0.8	0.8	1.8	1.8		
	Change-out distance	90	90	90	58	90	90	75	75	75	75		
	Tram distance	270	220	170	273	0	240	35	35	225	225		
	Recursion value	428	365	**260**	603	1800	4176	2060	1545	3840	2880		
Cuts Available for 7th cut		1	**2**	9	12	16	17	27	28	29	30		
	Bolting factor	1	1	10	1	4	2	4	4	2	2		
	Ventilation factor	1	1	1	0.5	2	2	2	1.5	2	1.5		
	Cable handling factor	1.25	1	0.8	2.25	1.8	1.8	1.8	1.8	1.8	1.8		
	Change-out distance	90	90	123	58	90	90	75	75	75	75		
	Tram distance	183	133	0	295	203	263	188	188	248	248		
	Recursion value	318	**223**	1225	361	3636	2250	3300	2475	2082	1562		
Cuts Available for 8th cut		**1**	8	9	12	16	17	27	28	29	30		
	Bolting factor	1	10	4	1	2	1	2	2	1	1		
	Ventilation factor	1	1	1	0.5	2	2	2	1.5	2	1.5		
	Cable handling factor	1	0.8	1.8	2.25	1.8	2.15	1.8	1.8	2.15	2.15		
	Change-out distance	90	123	123	58	90	90	75	75	75	75		
	Tram distance	133	0	165	345	253	313	238	238	298	298		
	Recursion value	**223**	1225	1678	417	2178	1524	2010	1508	1429	1072		
Cuts Available for 9th cut		7	8	9	**12**	16	17	27	28	29	30		
	Bolting factor	10	4	2	1	1	1	1	1	1	1		
	Ventilation factor	1	1	1	0.5	2	2	2	1.5	2	1.5		
	Cable handling factor	0.8	1.8	1.8	2.25	2.15	2.15	2.15	2.15	2.15	2.15		
	Change-out distance	123	123	123	58	90	90	75	75	75	75		
	Tram distance	0	165	215	395	303	363	288	288	348	348		
	Recursion value	1225	1678	1019	**473**	1481	1739	1386	1040	1644	1233		
Cuts Available for 10th cut		7	8	9	16	17	18	27	28	29	**30**	31	32
	Bolting factor	4	2	1	1	1	10	1	1	1	1	10	10
	Ventilation factor	1	1	1	2	2	2	2	1.5	2	1.5	2	1.5
	Cable handling factor	1.25	1.25	1.25	1.25	1	0.8	1.25	1.25	1	1	0.8	0.8
	Change-out distance	123	123	123	90	90	90	75	75	75	75	75	75
	Tram distance	428	378	328	305	245	0	290	290	230	230	35	35
	Recursion value	2628	1189	532	943	670	1800	875	656	610	**458**	2060	1545
Cuts Available for 11th cut		7	8	9	16	17	18	27	**28**	29	31	31	32
	Bolting factor	2	1	1	1	10	4	1	1	10	10	4	4
	Ventilation factor	1	1	1	2	2	2	2	1.5	2	1.25	2	1.5
	Cable handling factor	1.25	1.25	1.25	1	0.8	2	1	1	0.8	0.8	2	2
	Change-out distance	123	123	123	90	90	90	75	75	75	90	75	75
	Tram distance	363	313	263	240	50	245	225	225	35	0	230	230
	Recursion value	1151	513	451	660	2600	4640	600	**450**	2060	1125	4280	3210

Cuts	Available for 12th cut	7	8	**9**	16	17	18	27	29	29	31	31	32					
	Bolting factor	1	1	1	10	4	2	10	10	4	4	2	2					
	Ventilation factor	1	1	1	2	2	2	2	1.25	2	1.25	2	1.5					
	Cable handling factor	1.25	1.25	1	0.8	1.8	2	0.8	0.8	1.8	1.8	2	2					
	Change-out distance	123	123	123	90	90	90	75	90	75	90	75	75					
	Tram distance	303	253	203	50	240	305	35	0	225	240	290	290					
	Recursion value	501	438	**325**	2600	4176	2800	2060	1125	3840	2610	2620	1965					

Cuts	Available for 13th cut	7	**8**	15	16	17	18	26	27	27	29	29	31	31	32			
	Bolting factor	1	1	10	4	2	1	10	10	4	4	2	2	1	1			
	Ventilation factor	1	1	2	2	2	2	2	1.5	2	1.25	2	1.25	2	1.5			
	Cable handling factor	1.25	1	0.8	1.8	1.8	2.25	0.8	0.8	1.8	1.8	1.8	1.8	2.25	2.25			
	Change-out distance	123	123	155	90	90	90	140	140	75	90	75	90	75	75			
	Tram distance	248	198	0	235	295	360	35	35	220	235	280	295	345	345			
	Recursion value	432	**320**	3100	4104	2484	1800	3360	2520	3768	2565	2316	1553	1703	1277			

Cuts	Available for 14th cut	**7**	14	15	16	17	18	25	26	26	27	27	29	29	31	31	32	
	Bolting factor	1	10	4	2	1	1	10	10	4	4	2	2	1	1	1	1	
	Ventilation factor	1	2	2	2	2	2	2	1.5	2	1.5	2	1.25	2	1.25	2	1.5	
	Cable handling factor	1	0.8	1.8	1.8	2.15	2.25	0.8	0.8	1.8	1.8	1.8	1.8	2.15	2.15	2.25	2.25	
	Change-out distance	123	155	155	90	90	90	140	140	140	140	75	90	75	90	75	75	
	Tram distance	198	0	230	285	345	410	35	35	215	215	270	285	330	345	395	395	
	Recursion value	**320**	3100	4552	2412	1664	2025	3360	2520	4216	3162	2244	1508	1569	1040	1928	1446	

Cuts	Available for 15th cut	13	14	15	16	17	18	25	25	26	26	27	27	**29**	29	31	31	32
	Bolting factor	10	4	2	1	1	1	10	4	4	2	2	1	1	1	1	1	1
	Ventilation factor	2	2	2	2	2	2	1.5	2	1.5	2	1.5	2	1.25	2	1.25	2	1.5
	Cable handling factor	0.8	1.8	1.8	2.15	2.15	2.25	0.8	1.8	1.8	1.8	1.8	2.15	2.15	2.15	2.15	2.25	2.25
	Change-out distance	155	155	155	90	90	90	140	140	140	140	140	75	90	75	90	75	75
	Tram distance	0	230	280	335	395	460	35	215	215	265	265	320	335	380	395	445	445
	Recursion value	3100	4552	2636	1621	1879	2250	2520	4216	3162	2468	1851	1526	**1013**	1784	1174	2153	1614

Cuts	Available for 16th cut	13	14	15	**16**	17	18	25	25	26	26	27	27	31	31	32		
	Bolting factor	4	2	1	1	5	1	4	2	2	1	1	1	5	1	1		
	Ventilation factor	2	2	2	1	1	2	1.5	2	1.5	2	1.5	2	1.25	2	1.5		
	Cable handling factor	1.25	1.25	1.25	0.8	1.8	2	1.25	1.25	1.25	1.25	1.25	0.8	1.8	2	2		
	Change-out distance	155	155	155	90	90	90	140	140	140	140	140	75	90	75	75		
	Tram distance	370	320	270	85	275	340	355	305	305	255	255	70	275	325	325		
	Recursion value	4940	2220	985	**158**	2925	1540	3503	2085	1564	918	688	262	3656	1450	1088		

Cuts	Available for 17th cut	13	14	15	22	17	18	25	25	26	26	27	**27**	31	31	32		
	Bolting factor	2	1	1	10	1	1	2	1	1	1	1	5	1	1	1		
	Ventilation factor	2	2	2	1	1	2	1.5	2	1.5	2	1.5	0.5	1.25	2	1.5		
	Cable handling factor	1.25	1.25	1	0.8	1.8	2	1.25	1.25	1.25	1	1	0.8	1.8	2	2		
	Change-out distance	155	155	155	123	90	90	140	140	140	140	140	135	90	75	75		
	Tram distance	368	318	268	0	273	338	353	303	303	253	253	68	273	323	323		
	Recursion value	2458	1104	845	1225	581	1530	1742	1036	777	785	589	**473**	726	1440	1080		

Cuts	Available for 18th cut	13	14	15	22	**17**	18	25	25	26	26	31	31	32				
	Bolting factor	1	1	5	10	1	1	1	1	1	10	1	1	1				
	Ventilation factor	2	2	1	1	1	2	1.5	2	1.5	0.5	1.25	2	1.5				
	Cable handling factor	1.25	1.25	1	0.8	1.8	2	1.25	1.25	1.25	1	1.8	2	2				
	Change-out distance	155	155	155	123	90	90	140	140	140	130	90	75	75				
	Tram distance	365	315	265	113	270	335	350	300	300	20	270	320	320				
	Recursion value	1223	1098	2100	2125	**576**	1520	866	1030	773	750	720	1430	1073				

Cuts	Available for 19th cut	13	14	15	22	23	18	25	25	26	26	**31**	31	32				
	Bolting factor	1	1	1	2	10	1	1	1	1	4	1	1	1				
	Ventilation factor	2	2	1	1	1	2	1.5	2	1.5	0.5	1.25	2	1.5				
	Cable handling factor	1.25	1.25	1.25	1	0.8	2	1.25	1.25	1.25	1.25	0.8	2	2				
	Change-out distance	155	155	155	58	58	90	140	140	140	130	90	75	75				
	Tram distance	428	378	328	175	0	245	413	363	363	183	73	263	263				
	Recursion value	1379	1254	564	465	575	1160	983	1186	890	716	**185**	1200	900				

Cuts	Available for 20th cut	13	14	15	22	23	18	25	25	26	**26**	32						
	Bolting factor	1	1	1	1	4	5	1	1	1	2	5						
	Ventilation factor	2	2	1	1	1	1	1.5	2	1.5	0.5	0.75						
	Cable handling factor	1.25	1.25	1.25	1.25	0.8	2	1.25	1.25	1.25	1.25	2						
	Change-out distance	155	155	155	123	58	25	140	140	140	65	75						
	Tram distance	435	385	335	190	123	285	420	370	370	190	270						
	Recursion value	1398	1273	574	360	622	2975	998	1205	904	**303**	2306						

Cuts	Available for 21st cut	13	14	15	22	23	18	25	25	**32**								
	Bolting factor	1	1	5	1	2	1	1	5	1								
	Ventilation factor	2	1	1	2	2	1	1.5	2	0.75								
	Cable handling factor	2.15	2.15	0.8	1.8	1.8	2.25	2.15	2.15	2.15								
	Change-out distance	155	155	155	123	58	25	140	75	75								
	Tram distance	535	485	75	163	223	385	520	240	240								
	Recursion value	2611	1198	1075	830	1832	891	1887	5910	**443**								

Cuts	Available for 22nd cut	13	14	15	22	23	18	25	**25**	33								
	Bolting factor	1	1	1	1	1	5	1	1	10								
	Ventilation factor	1	1	1	2	2	1	1.5	0.5	0.5								
	Cable handling factor	2.15	2.15	2.15	2.15	1.8	0.8	2.15	2.15	0.8								
	Change-out distance	155	155	155	58	58	25	140	60	98								
	Tram distance	468	288	238	215	155	58	453	273	0								
	Recursion value	1160	773	666	1040	673	355	1669	**323**	488								

Cuts	Available for 23nd cut	13	14	15	22	23	**18**	33										
	Bolting factor	5	5	1	1	1	1	4										
	Ventilation factor	1	1	1	2	2	1	0.5										
	Cable handling factor	2.15	0.8	1.8	1.8	2.15	2.25	2.15										
	Change-out distance	90	90	90	58	58	25	98										
	Tram distance	585	535	485	213	273	305	313										
	Recursion value	6739	2590	963	880	1287	**711**	1539										